Millersville University

Setschenow Coefficients for Microbial Volatile Organic Compounds that Relate to Indoor Air Quality

A Senior Thesis Submitted to the Department of Chemistry & the University Honors College in Partial Fulfillment of the Requirements for the University & Departmental Honors Baccalaureate

Kelly J. Sprenkel

Millersville, Pennsylvania

March 2025

This is a placeholder page and not part of the original document submitted for approval.

The original page of this document containing the signatures of the parties involved has been extracted to protect their privacy.

Please contact the

Millersville University Archives & Special Collections

with any questions.

Placeholder version 1.0

Professor of Chemistry

Abstract

Microbial volatile organic compounds (mVOCs) are organic compounds commonly released by bacteria and fungi. These compounds relate to indoor air quality via Henry's Law and Setschenow coefficients. The Henry's Law and Setschenow coefficients are about the partitioning of compounds. Determining these coefficients will enable predictions about the behavior of these mVOCs in the indoor environment. The Setschenow equation and coefficients help to determine the solubility of a nonelectrolyte in an aqueous salt solution. Setschenow coefficients for many mVOCs in salt solutions are unknown, so to exam this and obtain experimental results, a shared headspace method was utilized. Six mVOCs and toluene were studied with six different salts present. It was hypothesized that the Setschenow coefficients for the salt solutions would correlate to the Hofmeister Series which shows the ionic pattern of salts precipitating in and out of proteins. Similar salt patterns have been seen elsewhere in nature.

To obtain the Setschenow coefficients, a shared headspace vial that contained various concentrations of salts and a 50/50 mix of store-bought olive oil and the mVOC(s) being studied was setup. Once the headspace reached equilibrium, an equal amount of the mixture from each concentration and a standard solution was extracted. Then, for each of the concentrations, a Gas Chromatography-Mass Spectrometry was obtained.

By taking the ratio of the area under the curve of the organic compound to the area under the curve of the standard and comparing it to the control 0.0M sample, Setschenow coefficients could be derived.

The Setschenow coefficients experimentally found were then used to build predictive models to determine Setschenow coefficients of salts and mVOCs that were not experimentally determined.

Acknowledgements

First and foremost, I would like to thank my thesis and research advisor, Dr. Albert, for his continued support over the past four years at Millersville University. Working with him throughout this process has truly been amazing, and his guidance has allowed me to grow both as a researcher and as a person. His guidance on this project has been instrumental in honing my research and professional skills for my future.

Next, I would like to thank Dr. Elioff for serving as my academic advisor and on my thesis committee. His guidance has allowed me to expand my interests both inside the department and in other areas. I would also like to thank Dr. Mbindyo for serving on my thesis committee and guiding me throughout this process.

Thank you to the Millersville University Chemistry Department for their support throughout these four years. I want to especially thank Dr. Mullen-Davis for allowing us to borrow a shaker plate to speed up the equilibrium, as well as Mr. Stephen Nolte for taking care of the GC-MS used in this experiment. I would also like to thank the Southeastern Pennsylvania Section of the American Chemical Society for funding my travel expenses to present this work. I would like to give a special thanks to Ms. Karen Murley, who graciously funds the Murley SURF. This allowed me to work on this project throughout the Summer 2023. She has allowed me to develop the skills necessary to move forward through my professional life.

Finally, I would like to thank all my friends and family; I truly could not have done this without them. I would like to thank Brooke Taylor and Natalie Landes specifically- from early morning classes to late night study sessions, we have shared in a lot of the joys and pain that college brings. I would also like to thank my parents for supporting me endlessly. They always believed in me, even when I didn’t believe in myself. Their encouragement kept me going.

Table of Contents

Introduction

Microbial volatile organic compounds (mVOCs) are a set of two thousand organic compounds that are formed and emitted by over one thousand microbial species, including bacteria and fungi through fermentation[1,2,3]. They are volatile due to their low molecular weight, low boiling point, and high vapor pressure[1]. These mVOCs are important in numerous chemical processes occurring in both natural and artificial environments. The organic compounds unique to microbial and their chemical properties are not very well understood[2].

In recent years, mVOCs for indoor air quality (IAQ) have gained attention, mainly due to modern humans spending a majority (approximately 90%) of their time indoors and the unique environment with restrained ventilation[4]. Mold is generally a sign of microbial growth in buildings[5,6]. MVOCs often emit an unpleasant smell and can penetrate weak barriers such as wallpaper[7,8,9]. Due to this, mVOCs can help identify sick building syndrome (SBS), and some mVOCs may be a risk factor in SBS[7]. While they do occur in small concentrations, they can pose a health threat when emitted by mold. Their unpleasant aromas can be the first warning sign of invisible mold[10].

Invisible mold is mold that cannot be seen by the human eye. This mold is often hidden behind wallpaper or under carpeting. In recent years, mVOCs have been turned to as the first sign of this mold. In some studies, the Environmental Relative Moldiness Index (ERMI) values, which is DNA-based methods of quantifying indoor molds, showed a high level of mold presence in homes where owners thought there was none[11,12,13,14]. ERMI was a metric created by the US Environmental Protection Agency (EPA) to quantify mold contamination in US homes[15,16].

Mold can pose health effects if exposed over a long period of time. There has been proven positive correlation between mold-infested homes and respiratory diseases including asthma, rhinitis, and several chronic lower respiratory diseases[17,18]. If exposed for a long period of time, mold can also decrease lung function[19]. There are also correlation between some mVOCs being emitted and health symptoms correlated with stress. Asthma is the most common chronic disease of children in the US. In a study done by Vesper et al[11], there was a correlation found between high ERMI values and homes of asthmatic children through three cities across the US. The biological mechanisms observed between molds and respiratory health remain unclear.

There is a wide range of mVOCs, including varying chain lengths and functional groups. Many of them are alcohols, ketones, esters, or enols that are between seven to ten carbons in length. For this experiment, the mVOCs looked at were 1-octene-3-ol, 3-octanone, 2-nonanone, 2-pentanone, chlorobenzene, and benzaldehyde[3] to look at varying functional groups as well as varying chain lengths (Figure 1). Toluene is also studied throughout the experiment to ensure the findings were accurate.

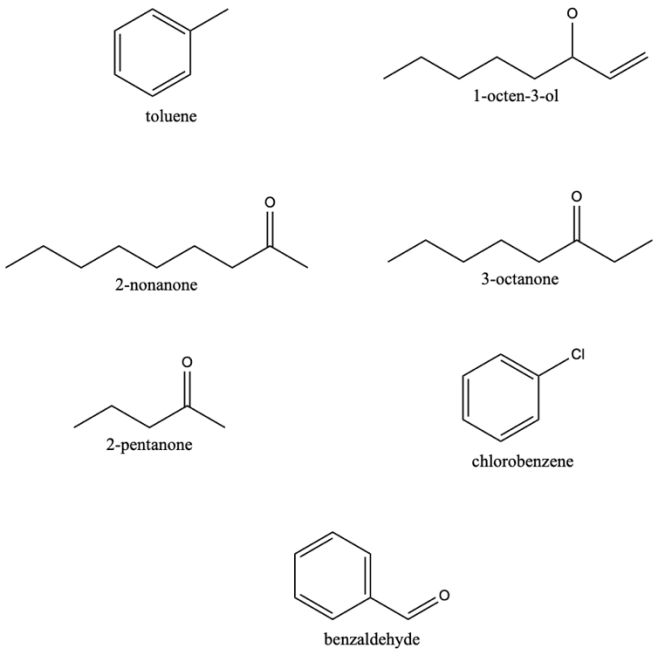

Figure 1. The seven mVOCs studied in this experiment.

Health risks of these mVOCs include allergy-like symptoms if exposed to for a long period of time[18]. These symptoms can include eye and skin irritation, nausea, headaches, and a decrease in lung capacity. In some extreme cases, mVOCs such as 1-octen-3-ol are known as a neurotoxin and can cause neurodegeneration[20,21].

To understand how these organic compounds affect the environment which, in turn, can help to predict pathways to human exposure, one can use indoor chemical partitioning. Indoor chemical partitioning is typically described by the water-air partition coefficient (K_{WA}) and the octanol-air partition coefficient (K_{OA}), which are the following equations, respectively[22]:

$$K_{WA} = \frac{C_W}{C_A}$$

$$K_{OA} = \frac{C_O}{C_A}$$

where C_W, C_A, and C_O are equilibrium concentrations of a certain species in aqueous, gas, and octanol phases, respectively.

From these equations, one can derive Henry's Law. Henry's Law states that the amount of a gas dissolved in liquid is proportional to its partial pressure above the liquid. Henry's Law is described by the following equation[23,24]:

$$K_H P^* = C$$

where P* is the partial pressure of the gas above the liquid, K_H is the Henry's Law Constant for the gas (which is equivalent to K_{WA}), and C is the concentration of the gas dissolved.

However, Henry's Law constants are generally only useful in pure water, not salt solutions. There are compilations of Henry's Law constants with water as a solvent, but a limited number of sources with salt water as the solvent[25]. Changes in salinity can cause the solubility of gases to change. In general, solubility of gases decrease with an increase of salinity, in an effect described by the Setschenow (or salting-out) equation and Setschenow coefficients[26]. Salting-out means that the electrolytes will decrease the solubility of neutral substances in water. The opposite (electrolytes increasing the solubility of neutral substances in water) is true for salting-in effects[30,31].

The Setschenow equation and coefficients help to determine the solubility of a nonelectrolyte in an aqueous salt solution. However, reliable Setschenow coefficients are lacking for most mVOCs[32,33,34]. Without the reliable Setschenow coefficients, one cannot properly understand environmental behavior and indoor chemical partitioning. This is important since most of the time in natural processes, there is salt dissolved in water, and it isn't just pure water. The Setschenow equation is as follows[26,27,28,29]:

$$\log\left(\frac{S_c}{S}\right) = -k_s c$$

where S_c is the area under the organic compound curve from a Gas Spectrometry chromatogram and S is the area under the water curve from the same chromatogram, C is the concentration of the salt, and k_s is the Setschenow coefficient. A positive k_s means that the salt is causing a salting-out effect, while a negative k_s value means that the salt is causing a salting-in effect. Many Setschenow coefficients of mVOCs are lacking, especially for salts other than NaCl.

While setting up this experiment, it was hypothesized that the salts being looked at will follow a similar trend to that of the Hofmeister Series. The Hofmeister Series is the pattern that salts that precipitate proteins follow. It is a specific ion series, and similar salt patterns have been seen elsewhere in nature (specifically in aqueous processes). The Hofmeister Series has been used to determine how ion specificity influences the critical micelle concentration of surfactants. This phenomenon has also been observed in the cloud point of polymers, the solubility of proteins and enzymes, colloids, and the surface tension of electrolyte solutions[37]. For the anions, the pattern is[35,36,37]

$$CO_3^{2-} > SO_4^{2-} > S_2O_3^{2-} > H_2PO_4^- > F^- > Cl^- > Br^- > NO_3^- > I^- > ClO_4^- > SCN^-$$

For the cations, the pattern is[36,37]

$$N(CH_3)_4^+ > NH_4^+ > Cs^+ > Rb^+ > K^+ > Na^+ > Li^+ > Ca^{2+} > Mg^{2+} > Zn^{2+} > Ba^{2+}$$

Anything that is left of Cl^- in the anion series and left of Na^+ in the cation series tends to salt out. Anything that is right of Cl^- in the anion series and right of Na^+ in the cation series tends to salt out. Cl^- and Na^+ ions can salt in or salt out[35,36,37].

Using this pattern, a range of anions and cations from across the Hofmeister Series were studied in this experiment. The salts selected were magnesium chloride, sodium chloride, sodium sulfate, sodium iodide, ammonium chloride, and sodium nitrate. Sodium chloride was selected and studied in both the cation and anion series.

The overarching goal of this project was to determine Setschenow coefficients for different mVOCs over a range of salts and salinities to determine if there is a correlation. This was done via gas chromatography-mass spectrometry (GC-MS) analysis. GC-MS is a type of instrumental analysis that can be used to study liquid samples, specifically those that are small and volatile. Analysis begins with the gas chromatograph, where the sample is vaporized into the gas phase and separated into its components. This is done via a capillary column coated with the stationary phase. The compounds are then propelled by an inert carrier gas, and the components are separated. Each compound will be eluted at different times, based on its boiling point and polarity (retention time)[38].

Once the components leave the GC portion of the instrument, they are ionized by the mass spectrometer using ionization sources. These ionized molecules are then accelerated through the instrument's mass analyzer. The ions are then separated based on their mass-to-charge (m/z) ratios[38].

The final step for GC-MS analysis is ion detection and analysis. Peak areas are proportional to the quantity of the corresponding compound for the gas chromatograph. When a complex sample is separated by GC-MS, it will produce multiple different peaks in the chromatogram (Figure 2), with each peak generating a unique mass spectrum. This mass spectrum can be used for compound identification. Using commercially available libraries of mass spectra, target analytes can be identified and quantified[38].

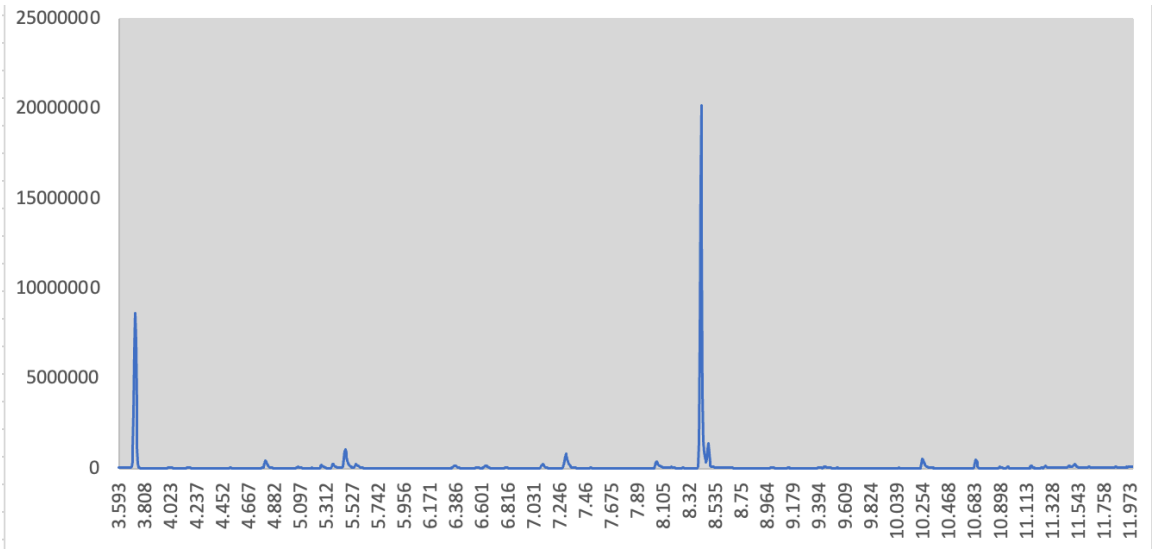

Figure 2. A sample gas chromatograph from this experiment.

Once the data was collected and analyzed, the findings were used along with a study done by Ni et al[40,42] to build two separate predictive models: one based on the K_{OW} of the mVOC and one based on the experimentally obtained value of the Setschenow coefficient for NaCl for each mVOC. A predictive model could provide a less tedious pathway to the determination of Setschenow coefficients than experimentally deriving them. With how little information there is about Setschenow coefficients, it is important to determine them with time-efficient and accurate means.

K_{OW} of many mVOCs are known and easily accessible through the mVOC database[39,40]. The predictive model used was similar to the ones found in Ni et al. The log K_{OW} of each mVOC (x-axis) were graphed against the experimental Setschenow coefficient (y-axis). This was repeated for all six salts, building a slightly different predictive model for all. Each followed the same basic formula:

$$K_{salt} = \log(K_{OW}) * m + b$$

where K_{salt} represented the Setschenow coefficient of the salt, m is the slope determined from the graph, and b is the y-intercept.

For the second predictive model, K_{salt} of the other five salts tried in this experiment were predicted using K_{NaCl} for each mVOC[42,43]. The Setschenow coefficients for NaCl are the most widely known of all the salts (with around 200 known Setschenow coefficients[41]). The K_{NaCl} of each mVOC (x-axis) were graphed against the experimental Setschenow coefficient for the other salt (y-axis). This allowed for development of a predictive model for each salt, with the general formula being as follows:

$$K_{salt} = K_{NaCl} * m + b$$

where m is the slope determined from the graph and b is the y-intercept. This information, combined with the information from the previous predictive model, can be used to predict Setschenow coefficients for various combinations of salts and mVOCs.

Experimental Methods: Shared Headspace Setup and Control Tests

For the experimental method, a shared headspace method was utilized. The shared headspace was a large vial with a screwed-on lid. The lid at the top had a rubber septum that allowed syringes to pass through it easily. Inside of this vial, there were four 4 mL vials without lids that contained 2.0 mL of liquid into each of them. A volumetric pipette was used to do this. These 4 mL vials were bounded together with two O-rings sized 19.

Inside the larger vial, a 50/50 mixture of the organic compound(s) and olive oil was added. The amount of this mixture ranged from 4mL to 10mL, with no effect on the results. Once this was added, the four 4mL vials bounded together were added into the larger vial and the vial was sealed.

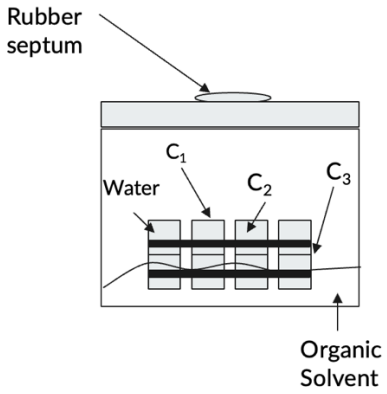

Figure 3. Schematic of basic shared headspace used for this experiment, where C_1, C_2, and C_3 represent the varying concentrations of salt added.

For the trials that took place within a day, the shared headspace was set it on a shaker plate for approximately 24 hours at 160 rpm to bring the solutions to equilibrium with the gas phase. The shared headspace method ensures that all of the solutions have the same partial pressure of the mVOC above them, allowing for accurate results. For the trials which took place with more time between loading the shared headspace and extracting the solutions, the shared headspace was left unshaken for about a week to reach equilibrium.

One concern was splashing within the shared headspace when shaking. To combat this, a control group was run to ensure there was no splashing. For the control group, each vial contained a different color of food dye, with deionized water filling the bottom (Figure 4). Readings were done of each color water with a spectrophotometer before and after shaking for 24 hours at 160 rpm. The readings showed no variance from before and after shaking, so it was conclusive of no splashing within the shared headspace.

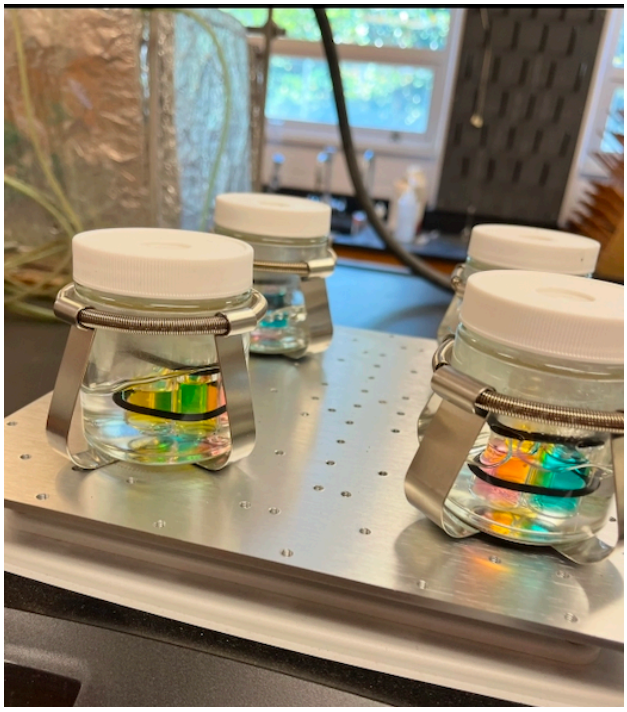

Figure 4. Food dye shared headspace.

For the first experiment, toluene was used as the organic solvent. To test the shared headspace method, only 2.0 mL of water was pipetted into the four vials. This control group was done to ensure the accuracy of the readings, as each should be similar. Seeing as they were similar readings, it was concluded that the shared headspace method that was proposed was a viable means to collect data. Toluene was also used as the first organic solvent to be tested with the salts. Toluene was repeated three times to make sure the results were reproduceable.

Stocks of the salts were all made at either 1.5 M or 2.0 M (Table 1). These stock solutions were used in every trial, and they were shaken before being used. For the salts that are 2.0 M stocks, the concentrations used for each trial were 0.0 M, 0.5 M, 1.0 M, and 1.5 M. For the salts that are 1.5 M, the concentrations used for each trial were 0.0 M, 0.5 M, and 1.0 M. The vial that would hold the 1.5 M was empty for these trials.

Salt	Concentration of Stock (M)
NaCl	1.966
NaI	1.972
$MgCl_2$	2.000
NH_4Cl	2.006
Na_2SO_4	1.496
$NaNO_3$	2.014

Table 1. Concentration of salt stocks for all six salts tested in this experiment.

For 1-octen-3-ol, 3-octanone, and 2-nonanone, each mVOC was the only mVOC used. For these three mVOCs, the trial was repeated three times to obtain multiple data points and minimize error.

For 2-pentanone and chlorobenzene, the mVOCs were added in equal parts to the olive oil, along with toluene. Toluene was present to ensure that the results would still be accurate for multiple mVOCs being studied at the same time. Toluene showed little variance when studied with other mVOCs, so it was concluded that adding multiple mVOCs was a viable means to study additional mVOCs time-efficiency. For these mVOCs, each salt was studied 1-3 times, depending on the salt and mVOC.

Benzaldehyde was the final mVOC studied. Benzaldehyde was studied by itself for one time per salt. Benzaldehyde was included to provide a broader range of functional groups and K_{OW} for the mVOCs studied.

Experimental Methods: Gas Chromatography-Mass Spectrometry Injections

To obtain Setschenow coefficients, all reactions, once equilibrium was reached, were injected and analyzed by gas chromatography-mass spectrometry (GC-MS, Agilent Technologies 5975 Inert XL Mass Selective detector). A standard solution of 4 mmol cyclohexene/hexanes was produced to ensure varying injection amounts would not cause the results to be skewed with cyclohexene serving as an internal standard. This also extracted the desired mVOC(s) from the remaining salt water in the compound. 0.5µL of the cyclohexene/hexanes standard was injected into 2 mL vials with a screw-top lid and rubber septum to prevent error. Then, 0.5µL of each sample was loaded into the vial with the standard and shaken. The organic portion of the sample was then loaded into the GC-MS (Figure 5).

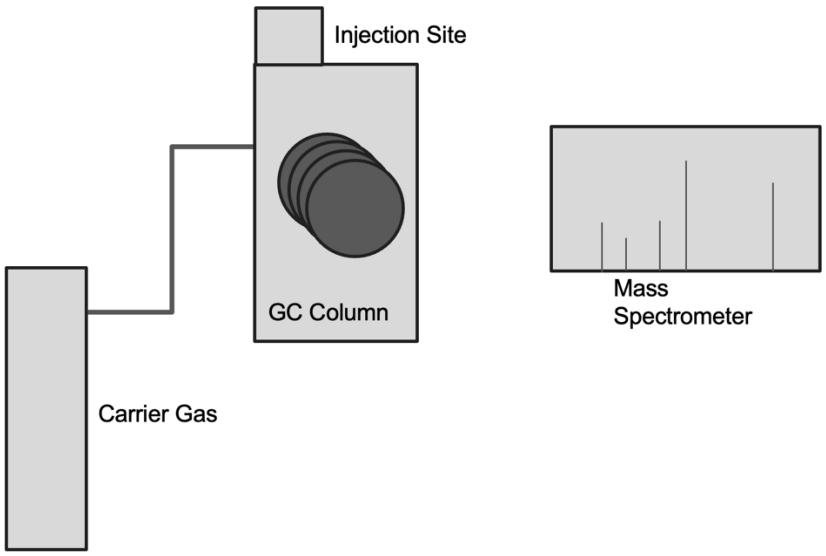

Figure 5. Basic schematic of GC-MS instrument.

The GC-MS data were recorded for twelve minutes to ensure the complete collection of data and to ensure that the data are not compromised from trial to trial. The initial 3.5 minutes were comprised of the solvent (hexanes), so a solvent delay of 3.5 minutes was added into the method.

Once the four readings for a shared headspace were complete, the data was collected and analyzed. Two data points were collected for each gas chromatograph- one for the area under the curve for the standard and one for the area under the curve for the target organic compound. The ratio between these areas were then found. This ratio for the 0.0M was then compared to the ratio for the other salts. To linearize this equation, the log was taken. These data points, collected for all three or four salinities were then plotted against the concentration of the salts.

Once these graphs were made for each salt and mVOC, the equation of the graphs were found. This equation is

$$\log\left(\frac{S_c}{S}\right) = -k_s c$$

where in this case, Sc is the area under the organic compound curve from a Gas Spectrometry graph, S is the area under the water curve from the same graph, c is the concentration of the salt, and k_s is the Setschenow coefficient. The Setschenow coefficients are the slopes of these graphs.

After the Setschenow coefficient for each salt and mVOC was obtained, the jack-knife error was taken[44]. In the jack-knife analysis, each datapoint was eliminated one term at a time. For example, the first datapoint in every trial was (0,0). This was eliminated, and then the slope was recalculated without this term. The term was then restored, and the next term was eliminated. This pattern continued until each datapoint was eliminated. The standard deviation was taken of the new slopes obtained. The standard error was taken by the following equation

$$Standard\ Error = \frac{n-1}{\sqrt{n}} * standard\ deviation$$

Where n is the number of data points in the trial. This was repeated for every trial run. These results were then used to build a predictive model for the Setschenow coefficients of other salts and other mVOCs, as outlined in the Introduction section and Ni et al.

Between experimental trials, the 2 mL vials were discarded and the shared headspace materials were rinsed with water and acetone.

Results and Discussion

All results were obtained using the procedures outlined in the Experimental Methods section. For the following figures (Figures 6-21 and Tables 2-15), the Setschenow coefficients are determined from the gas chromatographs. The error bars were determined by jack-knife analysis[44].

The Setschenow coefficients for chloride for 2-pentanone was determined in the following way. All other graphs can be found in the Appendix (pages 53-72). First, there were two different trials run as outlined in the Experimental Methods Section (pages 12-17). Each of these trials had four different concentrations for the salt (0.000 M, 0.492 M, 0.983 M, and 1.475 M). For each concentration, a gas chromatograph was obtained with the areas under the curve for the internal standard and the desired organic compound (in this case 2-pentanone). A ratio of the area under the curve for 2-pentatone to the area under the curve for the internal standard was then found. This ratio for the various concentrations (S_C) was then divided by the ratio for the 0.00 M (S). The log of this value (S_C/S or A) was then determined. This is the value for the left-hand side of Setschenow equation, as seen below.

$$\log\left(\frac{S_C}{S}\right) = -k_s c$$

This value was then plotted for each value of log (A) versus the concentration of the salt (Figure 6). The graph was then fitted with a linear equation, and the negative value of the slope is the Setschenow equation.

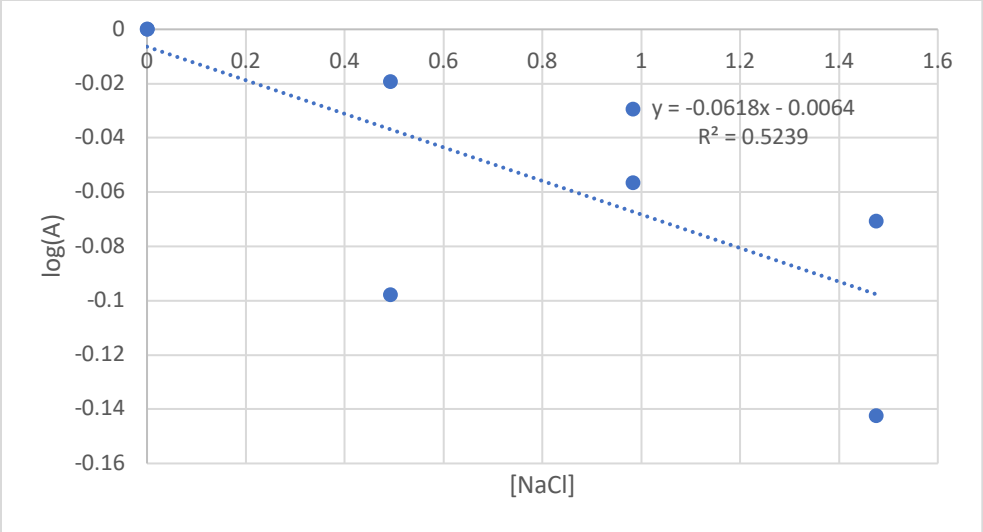

Figure 6. log(A) vs. [NaCl] for 2-pentanone.

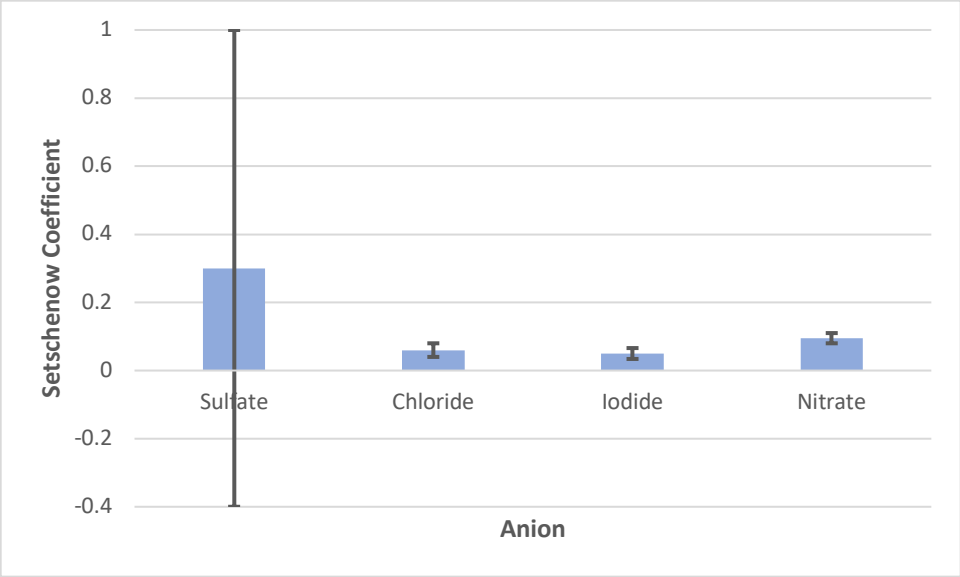

Figure 7. Comparison of 2-Pentanone Setschenow Coefficients for Anions with Error Bars

Anion	Setschenow Coefficients (1/M)
Sulfate	0.3 ± 0.7
Chloride	0.06 ± 0.02
Iodide	0.050 ± 0.016
Nitrate	0.095 ± 0.015

Table 2. Comparison of 2-Pentanone Setschenow Coefficients for Anions with Jack-Knife Errors

Figure 7 shows the comparison of 2-pentanone Setschenow coefficients for anions. The Setschenow coefficients show that sulfate ions have the biggest salting-out effect, while iodide ions have the smallest salting-out effect. Nitrate anions had the second largest salting-out effect, while chloride anions had the second smallest salting-out effect. This follows the same pattern as the Hofmeister Series. Table 2 shows these Setschenow coefficients with errors produced from the Jack-Knife method. It is important to note the very large margin of error for the sulfate ion.

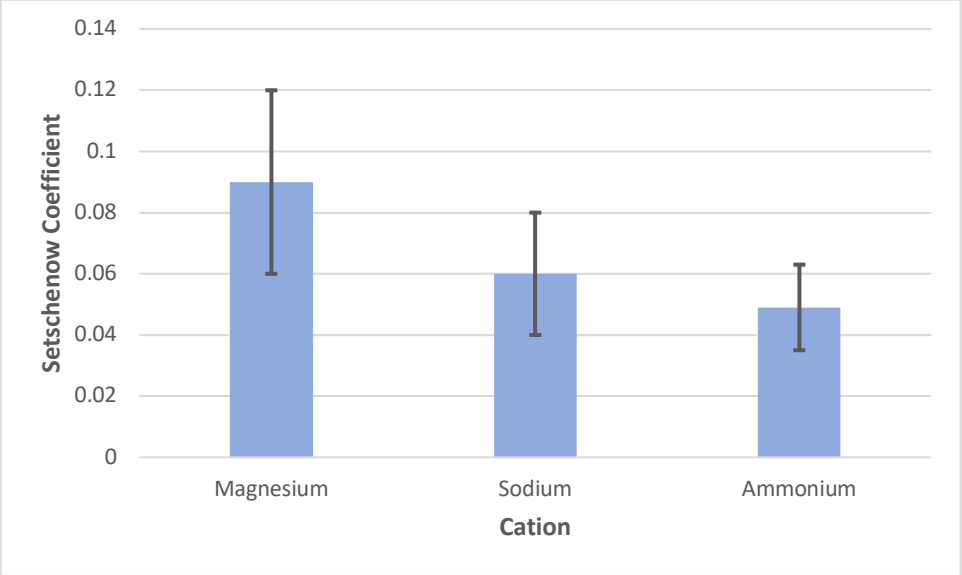

Figure 8. Comparison of 2-Pentanone Setschenow Coefficients for Cations with Error Bars

Cation	Setschenow Coefficients (1/M)
Magnesium	0.09 ± 0.03
Sodium	0.06 ± 0.02
Ammonium	0.049 ± 0.014

Table 3. Comparison of 2-Pentanone Setschenow Coefficients for Cations with Jack-Knife errors

Figure 8 shows the comparison of 2-pentanone Setschenow coefficients for cations. The Setschenow coefficients show that magnesium ions have the biggest salting-out effect, while ammonium ions have the smallest salting-out effect. This varies from the Hofmeister series, where ammonium ions have the largest salting-out effect and magnesium ions have the smallest salting-out effect.

Table 3 shows these Setschenow coefficients with errors produced from the Jack-Knife method. There was a relatively high level of error for all three cations, which may explain the inconsistencies between this data set and the Hofmeister series.

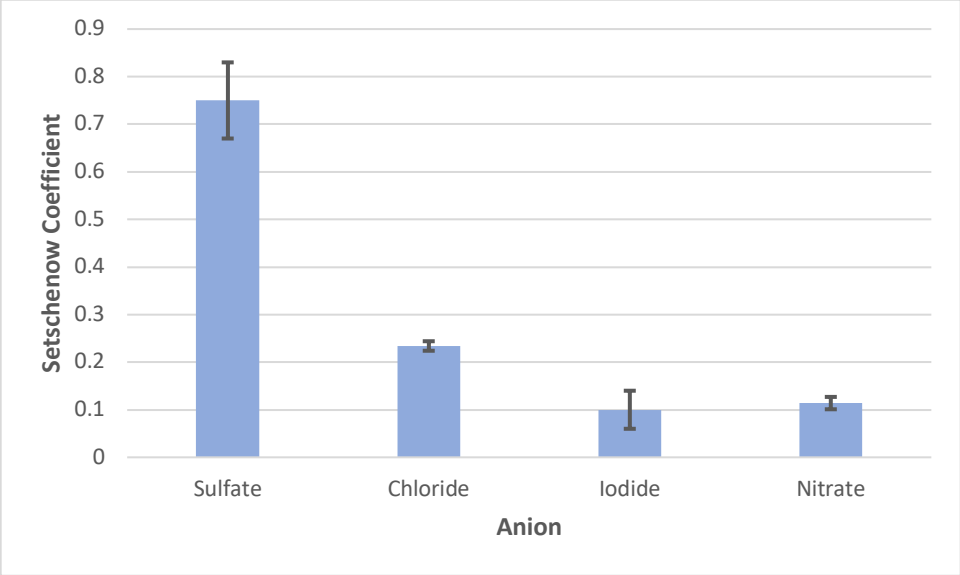

Figure 9. Comparison of 3-Octanone Setschenow Coefficients for Anions with Error Bars

Anion	Setschenow Coefficients (1/M)
Sulfate	0.75 ± 0.08
Chloride	0.234 ± 0.010
Iodide	0.10 ± 0.04
Nitrate	0.114 ± 0.013

Table 4. Comparison of 3-Octanone Setschenow Coefficients for Anions with Jack-Knife errors

Figure 9 shows the comparison of 3-octanone Setschenow coefficients for anions. The Setschenow coefficients show that sulfate ions have the biggest salting-out effect, while iodide ions have the smallest salting-out effect. Chloride anions had the second largest salting-out effect, while nitrate anions had the second smallest salting-out effect. This agrees with the Hofmeister series.

Table 4 shows these Setschenow coefficients with errors produced from the Jack-Knife method. These errors, which are relatively small, help confirm that these anions follow the Hofmeister series.

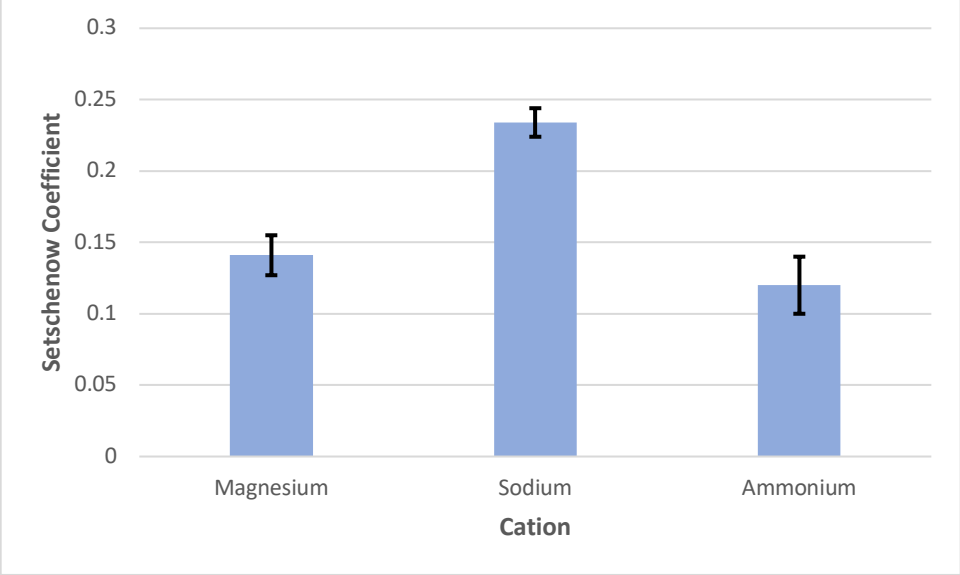

Figure 10. Comparison of 3-Octanone Setschenow Coefficients for Cations with Error Bars

Cation	Setschenow Coefficients (1/M)
Magnesium	0.141 ± 0.014
Sodium	0.234 ± 0.010
Ammonium	0.12 ± 0.02

Table 5. Comparison of 3-Octanone Setschenow Coefficients for Cations with Jack-Knife errors

Figure 10 shows the comparison of 3-octanone Setschenow coefficients for cations. The Setschenow coefficients show that sodium ions have the largest salting-out effect, while ammonium ions have the smallest salting-out effect. This varies from the Hofmeister series, where ammonium ions have the largest salting-out effect and magnesium ions have the smallest salting-out effect.

Table 5 shows these Setschenow coefficients with errors produced from the Jack-Knife method. There was relatively small errors, which most likely means 3-octanone Setschenow coefficients for cations do not follow the Hofmeister series for cations.

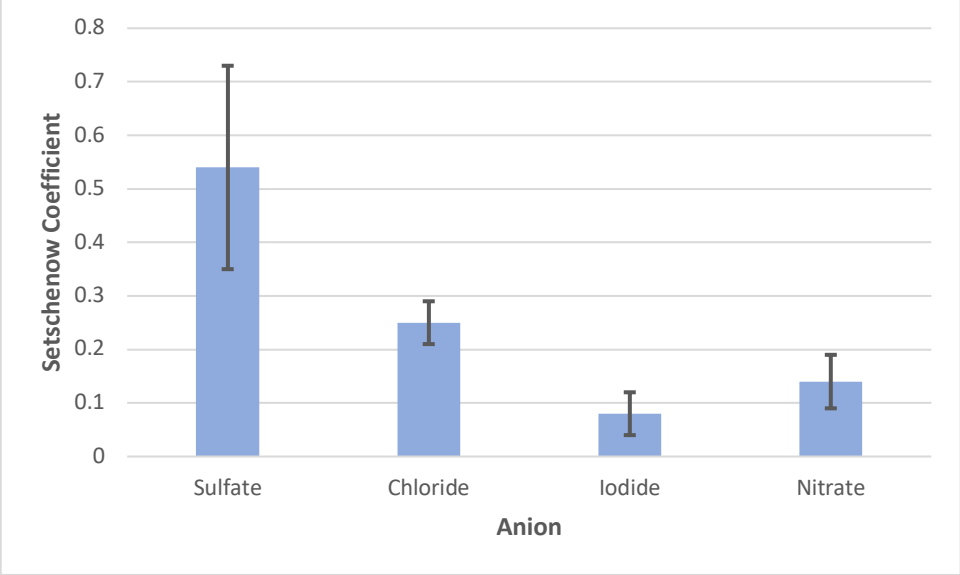

Figure 11. Comparison of 2-Nonanone Setschenow Coefficients for Anions with Error Bars

Anion	Setschenow Coefficients (1/M)
Sulfate	0.54 ± 0.19
Chloride	0.25 ± 0.04
Iodide	0.08 ± 0.04

Nitrate	0.14 ± 0.05

Table 6. Comparison of 2-Nonanone Setschenow Coefficients for Anions with Jack-Knife errors

Figure 11 shows the comparison of 2-nonanone Setschenow coefficients for anions. The Setschenow coefficients show that sulfate ions have the biggest salting-out effect, while iodide ions have the smallest salting-out effect. Chloride anions had the second largest salting-out effect, while nitrate anions had the second smallest salting-out effect. This agrees with the Hofmeister series.

Table 6 shows these Setschenow coefficients with errors produced from the Jack-Knife method. These errors, which are relatively small, help confirm that these anions follow the Hofmeister series.

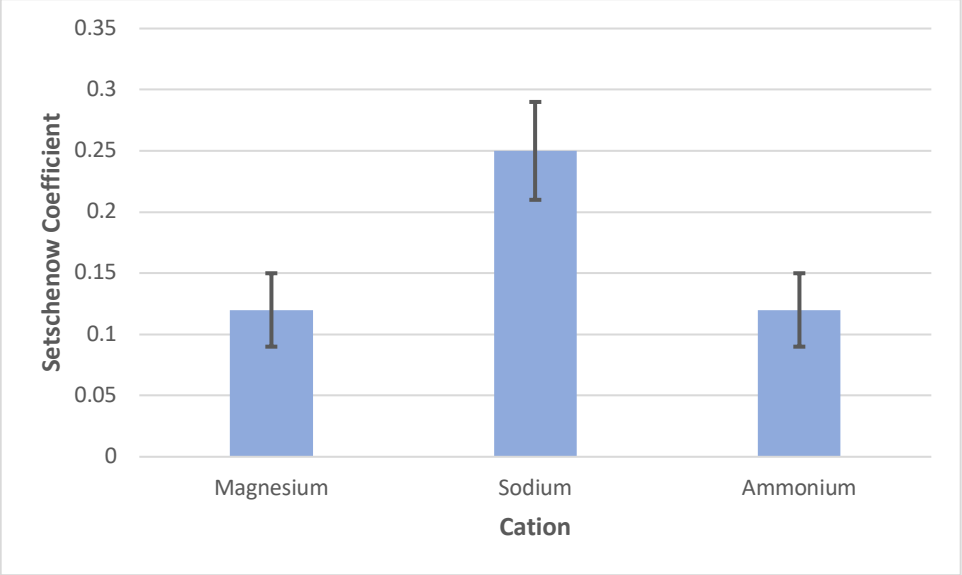

Figure 12. Comparison of 2-Nonanone Setschenow Coefficients for Cations with Error Bars

Cation	Setschenow Coefficients (1/M)
Magnesium	0.12 ± 0.03
Sodium	0.25 ± 0.04

Ammonium	0.12 ± 0.03

Table 7. Comparison of 2-Nonanone Setschenow Coefficients for Cations with Jack-Knife errors

Figure 12 shows the comparison of 2-nonanone Setschenow coefficients for cations. The Setschenow coefficients show that sodium ions have the biggest salting-out effect, while both ammonium ions and magnesium ions have the same salting-out effect. This varies from the Hofmeister series, where ammonium ions have the largest salting-out effect and magnesium ions have the smallest salting-out effect.

Table 7 shows these Setschenow coefficients with errors produced from the Jack-Knife method. There was relatively small errors, which most likely means 2-nonanone Setschenow coefficients for cations do not follow the Hofmeister series for cations.

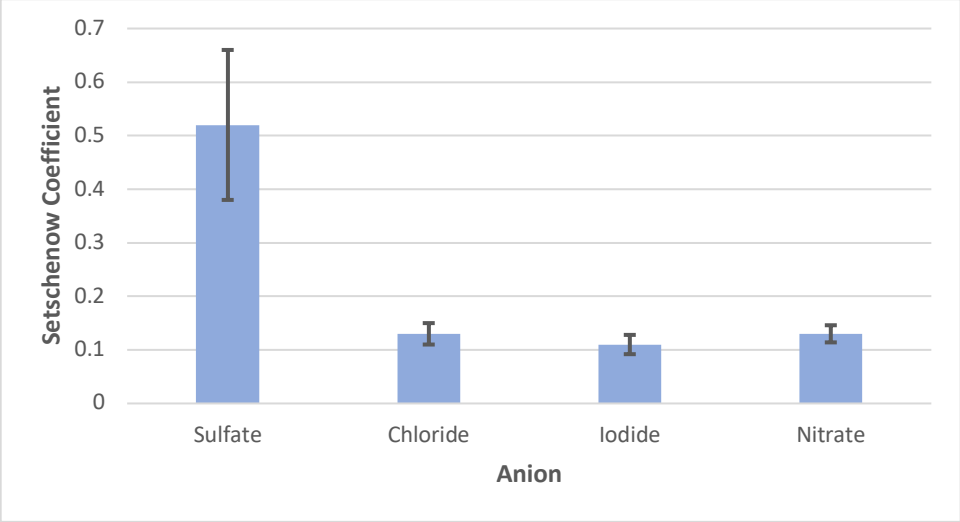

Figure 13. Comparison of Toluene Setschenow Coefficients for Anions with Error Bars

Anion	Setschenow Coefficients (1/M)
Sulfate	0.52 ± 0.14
Chloride	0.13 ± 0.02

Iodide	0.1100 ± 0.0018
Nitrate	0.13 ± 0.08

Table 8. Comparison of Toluene Setschenow Coefficients for Anions with Jack-Knife errors

Figure 13 shows the comparison of toluene Setschenow coefficients for anions. The Setschenow coefficients show that sulfate ions have the biggest salting-out effect, while iodide ions have the smallest salting-out effect. Chloride anions and nitrate ions both had the same Setschenow coefficient. This varies slightly from the Hofmeister series, but the errors (Table 8) are a possible explanation.

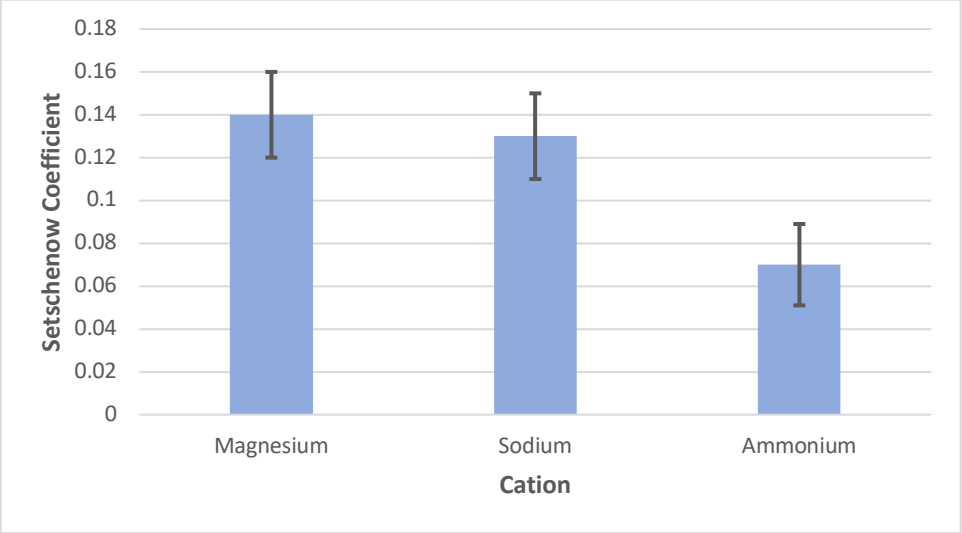

Figure 14. Comparison of Toluene Setschenow Coefficients for Cations with Error Bars

Cation	Setschenow Coefficients (1/M)
Magnesium	0.14 ± 0.02
Sodium	0.13 ± 0.02
Ammonium	0.070 ± 0.019

Table 9. Comparison of Toluene Setschenow Coefficients for Cations with Jack-Knife errors

Figure 14 shows the comparison of toluene Setschenow coefficients for cations. The Setschenow coefficients show that magnesium ions have the biggest salting-out effect, while ammonium ions have the smallest salting-out effect. This varies from the Hofmeister series, where ammonium ions have the largest salting-out effect and magnesium ions have the smallest salting-out effect.

Table 9 shows these Setschenow coefficients with errors produced from the Jack-Knife method. There was relatively small errors, which most likely means 1-octen-3-ol Setschenow coefficients for cations does not follow the Hofmeister series for cations.

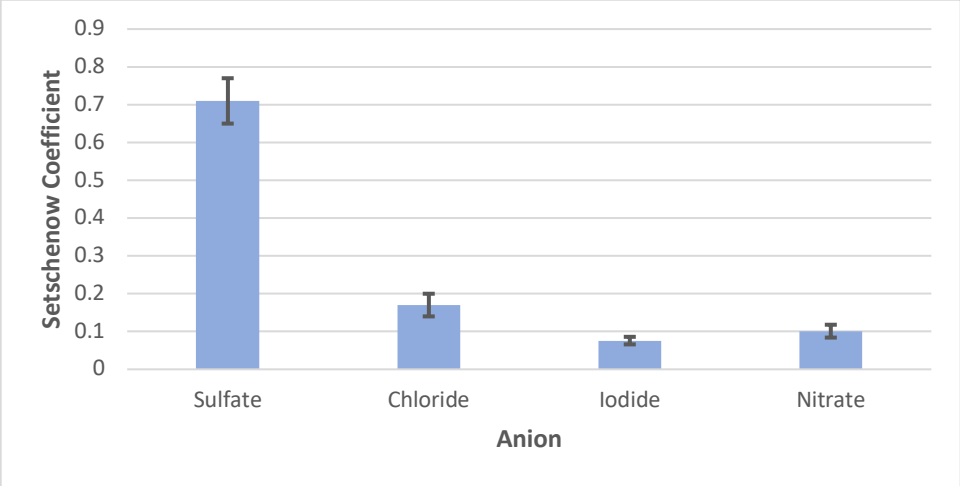

Figure 15. Comparison of 1-Octen-3-ol Setschenow Coefficients for Anions with Error Bars

Anion	Setschenow Coefficients (1/M)
Sulfate	0.71 ± 0.06
Chloride	0.17 ± 0.03
Iodide	0.076 ± 0.010
Nitrate	0.101 ± 0.017

Table 10. Comparison of 1-Octen-3-ol Setschenow Coefficients for Anions with Jack-Knife errors

Figure 15 shows the comparison of 1-octen-3-ol Setschenow coefficients for anions. The Setschenow coefficients show that sulfate ions have the biggest salting-out effect, while iodide ions have the smallest salting-out effect. Chloride anions had the second largest salting-out effect, while nitrate anions had the second smallest salting-out effect. This agrees with the Hofmeister series.

Table 10 shows these Setschenow coefficients with errors produced from the Jack-Knife method. These errors, which are relatively small, help confirm that these anions follow the Hofmeister series.

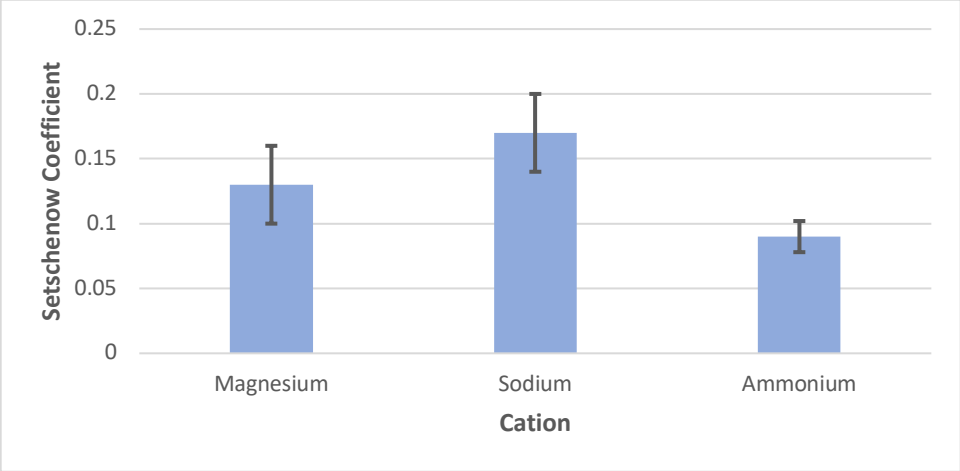

Figure 16. Comparison of 1-Octen-3-ol Setschenow Coefficients for Cations with Error Bars

Cation	Setschenow Coefficients (1/M)
Magnesium	0.13 ± 0.03
Sodium	0.17 ± 0.03
Ammonium	0.090 ± 0.012

Table 11. Comparison of 1-Octen-3-ol Setschenow Coefficients for Cations with Jack-Knife errors

Figure 16 shows the comparison of 1-octen-3-ol Setschenow coefficients for cations. The Setschenow coefficients show that sodium ions have the biggest salting-out effect, while ammonium ions have the smallest salting-out effect. This varies from the Hofmeister series, where ammonium ions have the largest salting-out effect and magnesium ions have the smallest salting-out effect.

Table 11 shows these Setschenow coefficients with errors produced from the Jack-Knife method. There was relatively small errors, which most likely means 1-octen-3-ol Setschenow coefficients for cations does not follow the Hofmeister series for cations.

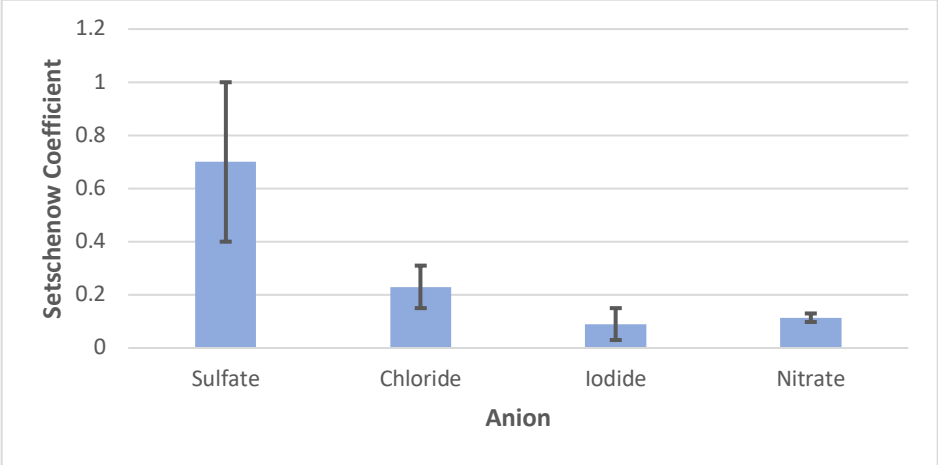

Figure 17. Comparison of Chlorobenzene Setschenow Coefficients for Anions with Error Bars

Anion	Setschenow Coefficients (1/M)
Sulfate	0.7 ± 0.3
Chloride	0.23 ± 0.08
Iodide	0.09 ± 0.06
Nitrate	0.114 ± 0.016

Table 12. Comparison of Chlorobenzene Setschenow Coefficients for Anions with Jack-Knife errors

Figure 17 shows the comparison of chlorobenzene Setschenow coefficients for anions. The Setschenow coefficients show that sulfate ions have the biggest salting-out effect, while iodide ions have the smallest salting-out effect. Chloride anions had the second largest salting-out effect, while nitrate anions had the second smallest salting-out effect. This agrees with the Hofmeister series.

Table 12 shows these Setschenow coefficients with errors produced from the Jack-Knife method. The errors are relatively small, except for the sulfate anion. However, this error may decrease if more experiments are run, due to a limited number of experiments run on chlorobenzene.

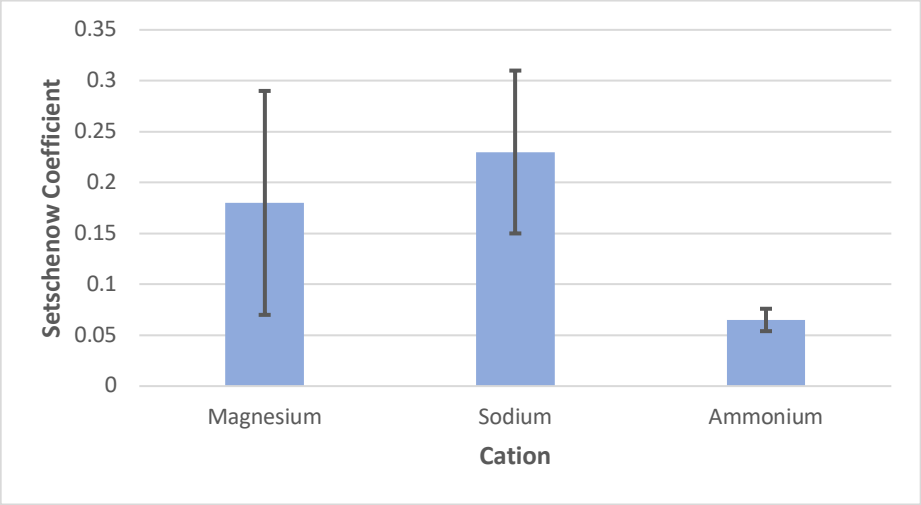

Figure 18. Comparison of Chlorobenzene Setschenow Coefficients for Cations with Error Bars

Cation	Setschenow Coefficients (1/M)
Magnesium	0.18 ± 0.11
Sodium	0.23 ± 0.08

Ammonium	0.065 ± 0.011

Table 13. Comparison of Chlorobenzene Setschenow Coefficients for Cations with Jack-Knife errors

Figure 18 shows the comparison of chlorobenzene Setschenow coefficients for cations. The Setschenow coefficients show that sodium ions have the largest salting-out effect, while ammonium ions have the smallest salting-out effect. This varies from the Hofmeister series, where ammonium ions have the largest salting-out effect and magnesium ions have the smallest salting-out effect.

Table 13 shows these Setschenow coefficients with errors produced from the Jack-Knife method. There is evidence of high error in these trials. However, a limited number of experiments were run on chlorobenzene. These errors may not fully explain the difference, and more trials need to be run.

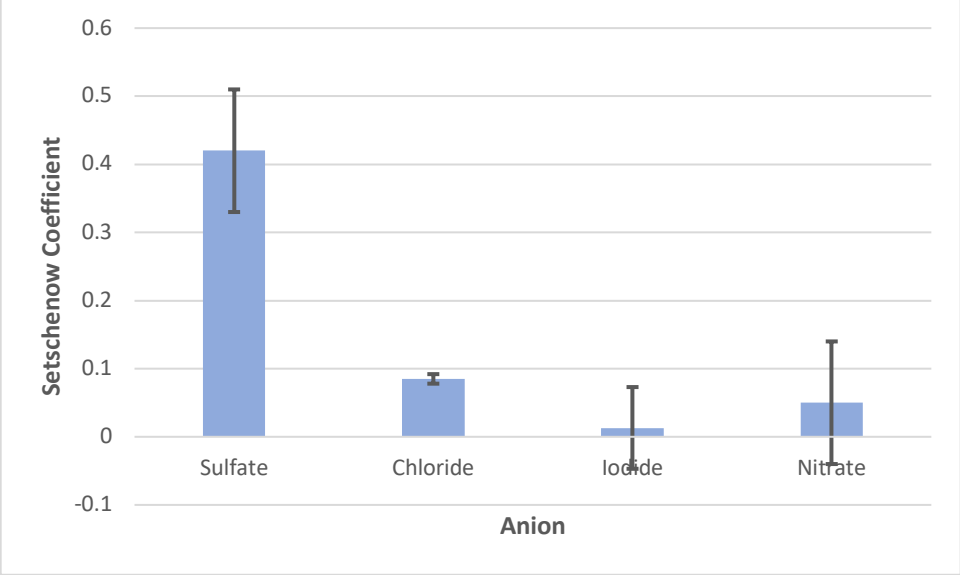

Figure 19. Comparison of Benzaldehyde Setschenow Coefficients for Anions with Error Bars

Anion	Setschenow Coefficients (1/M)
Sulfate	0.42 ± 0.09
Chloride	0.085 ± 0.007
Iodide	0.013± 0.06
Nitrate	0.05 ± 0.09

Table 14. Comparison of Benzaldehyde Setschenow Coefficients for Anions with Jack-Knife errors

Figure 19 shows the comparison of benzaldehyde Setschenow coefficients for anions. The Setschenow coefficients show that sulfate ions have the biggest salting-out effect, while iodide ions have the smallest salting-out effect. Chloride anions had the second largest salting-out effect, while nitrate anions had the second smallest salting-out effect. This agrees with the Hofmeister series.

Table 14 shows these Setschenow coefficients with errors produced from the Jack-Knife method. The errors can be especially large, particularly for iodide and nitrate. However, this error may decrease if more experiments are run, due to a limited number of experiments run on benzaldehyde.

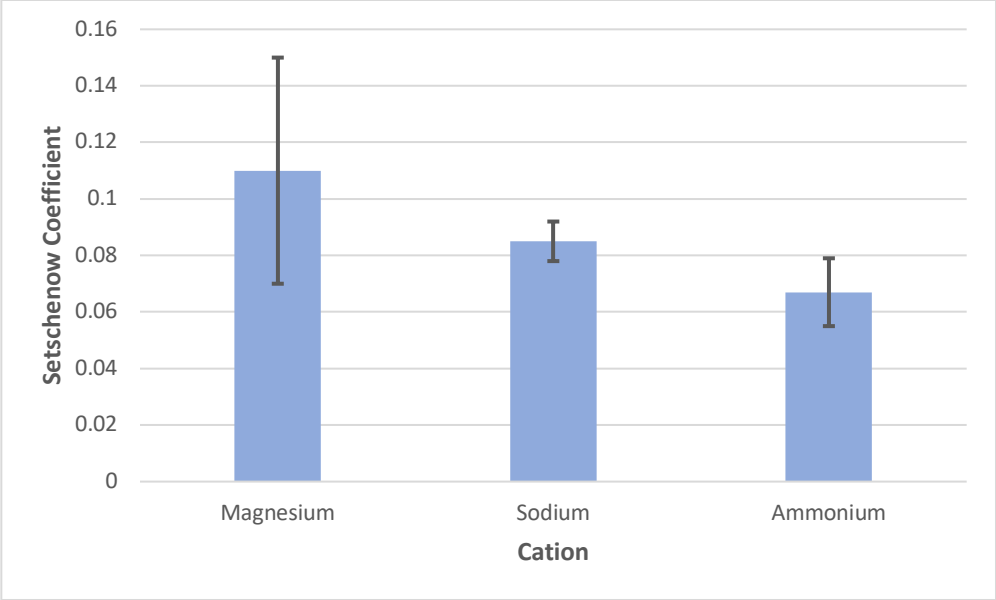

Figure 20. Comparison of Benzaldehyde Setschenow Coefficients for Cations with Error Bars

Cation	Setschenow Coefficients (1/M)
Magnesium	0.11 ± 0.04
Sodium	0.085 ± 0.007
Ammonium	0.067 ± 0.012

Table 15. Comparison of Benzaldehyde Setschenow Coefficients for Cations with Jack-Knife errors

Figure 20 shows the comparison of benzaldehyde Setschenow coefficients for cations. The Setschenow coefficients show that magnesium ions have the biggest salting-out effect, while ammonium ions have the smallest salting-out effect. This varies from the Hofmeister series, where ammonium ions have the largest salting-out effect and magnesium ions have the smallest salting-out effect.

Table 15 shows these Setschenow coefficients with errors produced from the Jack-Knife method. For magnesium, there is a large margin of error. However, a limited number of

experiments were run on benzaldehyde. These errors may not fully explain the difference, and more trials need to be run.

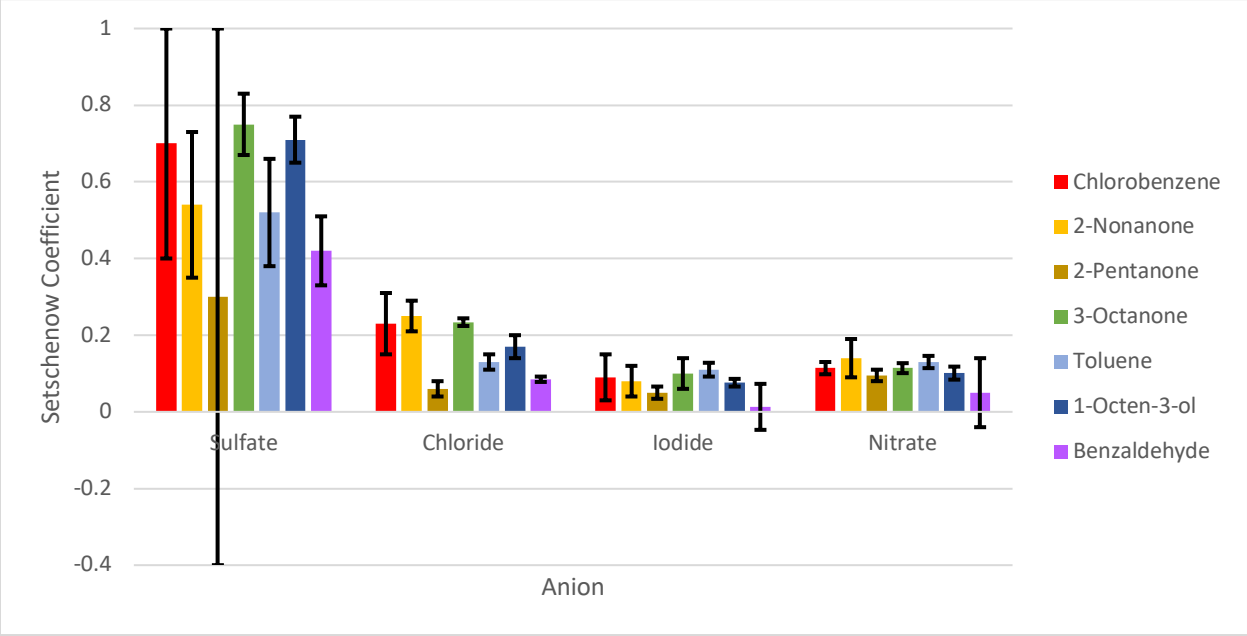

Figure 21. Comparison of All Setschenow Coefficients for Anions with Error Bars

Figure 21 shows the comparison of all Setschenow coefficients for the anions. From this figure, it is clear to see that the sulfate ion caused the largest Setschenow coefficients for all seven mVOCs studied. Chloride ions also produced larger Setschenow coefficients for the mVOCs, except for 2-pentanone and benzaldehyde. Iodine ions produced a larger Setschenow coefficients for benzaldehyde compared to the other mVOCs. Apart from benzaldehyde and 2-pentanone, iodide and nitrate produced comparable Setschenow coefficients. The five other mVOCs (chlorobenzene, 2-nonanone, 3-octanone, 1-octen-3-ol, and toluene) all follow the Hofmeister Series for anions.

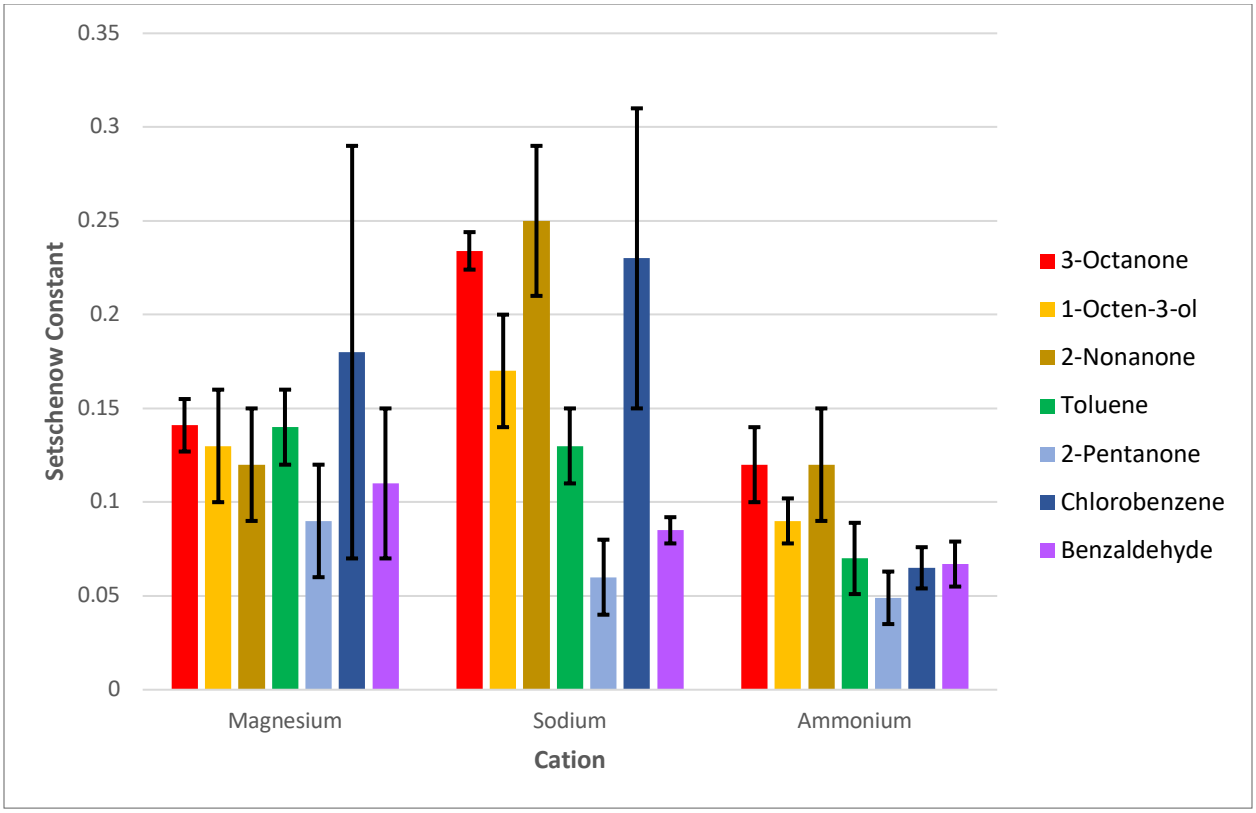

Figure 22. Comparison of All Setschenow Coefficients for Cations with Error Bars

Figure 22 shows the comparison of all Setschenow coefficients for the cations. From this figure, it is clear to see that the sodium ion caused the largest Setschenow coefficients for five of the seven mVOCs studied, except for 2-pentanone and toluene. The other two cations (magnesium and ammonium) produce comparable Setschenow coefficients. For the other two mVOCs, magnesium was the highest, with sodium being the second largest. However, there is large error margins for some of the magnesium and sodium trials, as evident from Figure 21.

The following prediction curves (Figures 23-28) are based on the K_{OW} of the mVOCs studied. The equations determined were from the linear line of best fit for the seven data points collected for each salt. While the lines are not a perfect fit for the data, they can provide a semi-accurate prediction for mVOCs not yet studied.

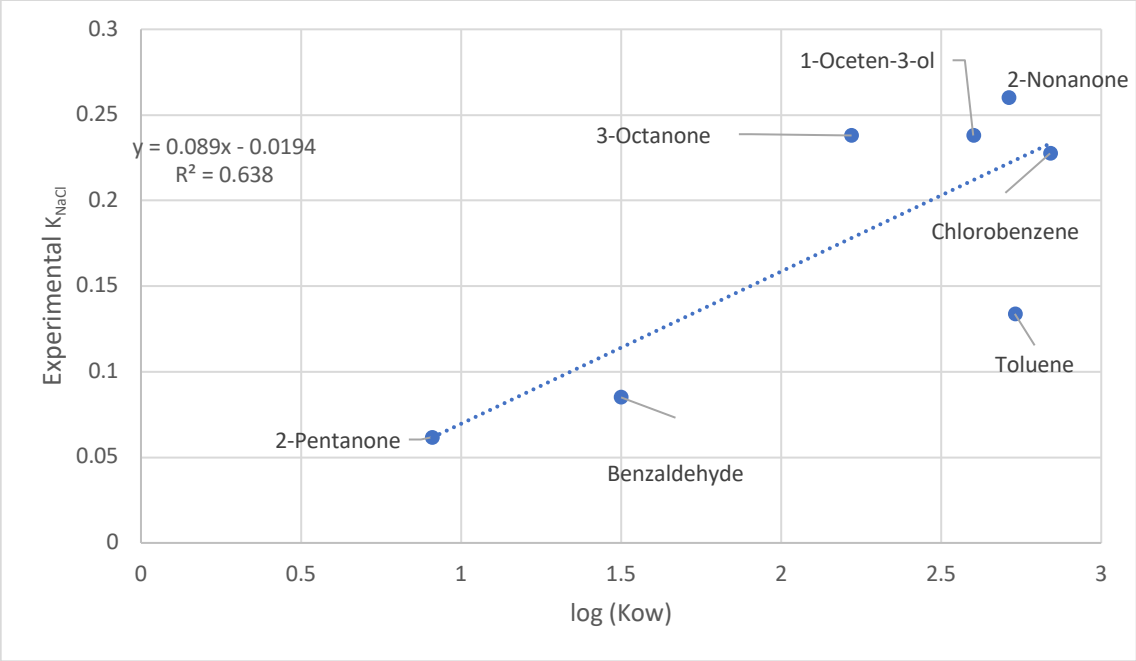

Figure 23. Prediction Curve for any mVOC's K_{NaCl} based on log(K_{OW}) and experimental K_{NaCl} for mVOCs studied. To determine K_{NaCl} for any mVOC, the equation derived from the curve, $K_{NaCl} = 0.089log(K_{OW}) - 0.0194$, can be used.

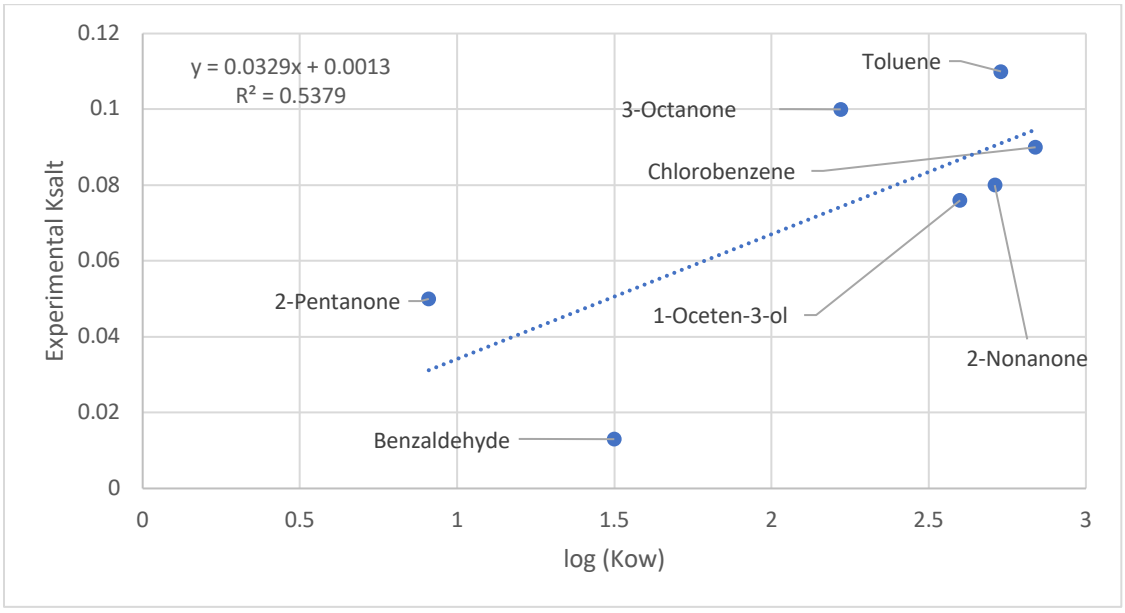

Figure 24. Prediction Curve for any mVOC's K_{NaI} based on log(K_{OW}) and experimental K_{NaI} for the mVOCs studied. To determine K_{NaI} for any mVOC, the equation derived from the curve, $K_{NaI} = 0.0329log(K_{OW}) + 0.0013$, can be used.

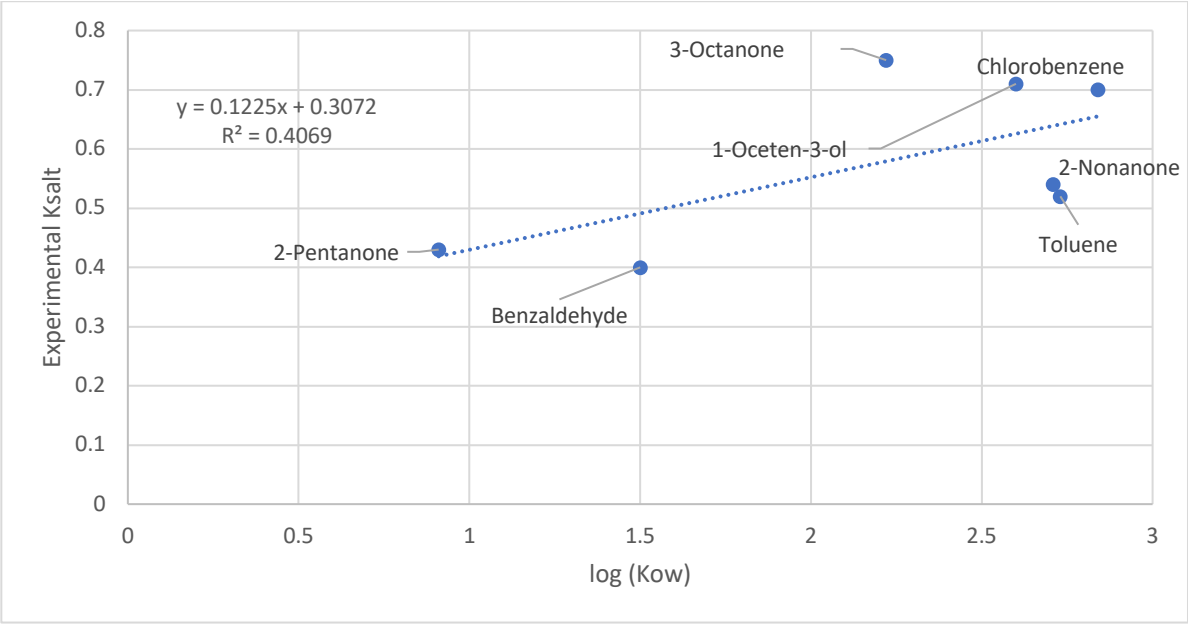

Figure 25. Prediction Curve for any mVOC's K_{Na2SO4} based on log(K_{OW}) and experimental K_{Na2SO4} for the mVOCs studied. To determine K_{Na2SO4} for any mVOC, the equation derived from the curve, $K_{Na2SO4} = 0.1225log(K_{OW}) + 0.3072$, can be used.

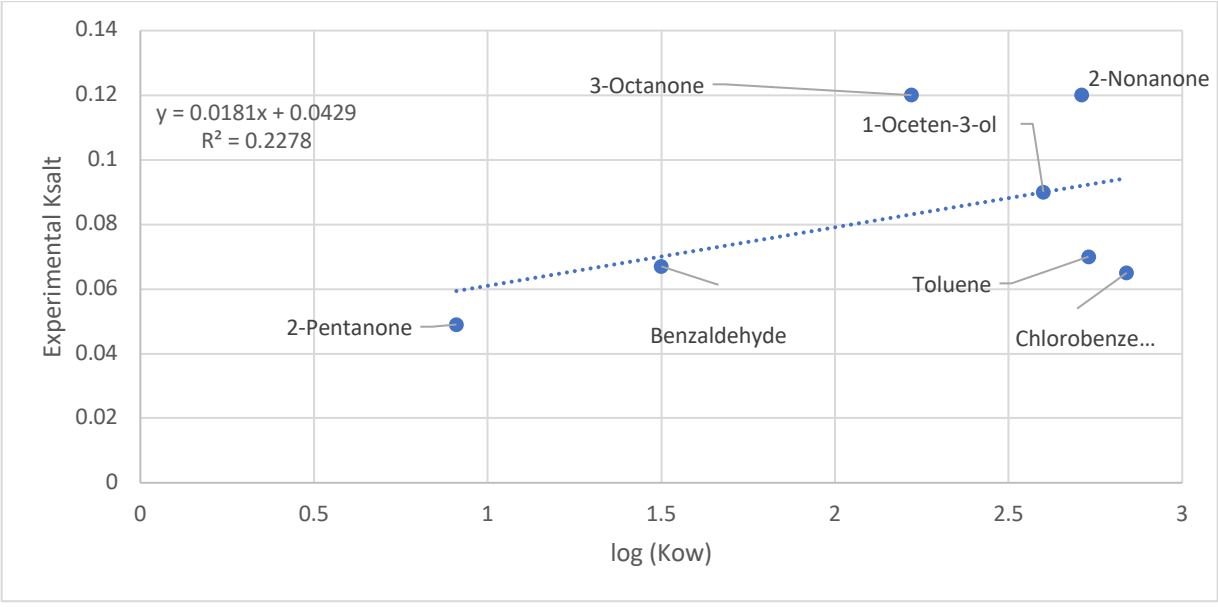

Figure 26. Prediction Curve for any mVOC's K_{NH4Cl} based on log(K_{OW}) and experimental K_{NH4Cl} for the mVOCs studied. To determine K_{NH4Cl} for any mVOC, the equation derived from the curve, $K_{NH4Cl} = 0.0181log(K_{OW}) + 0.0429$, can be used.

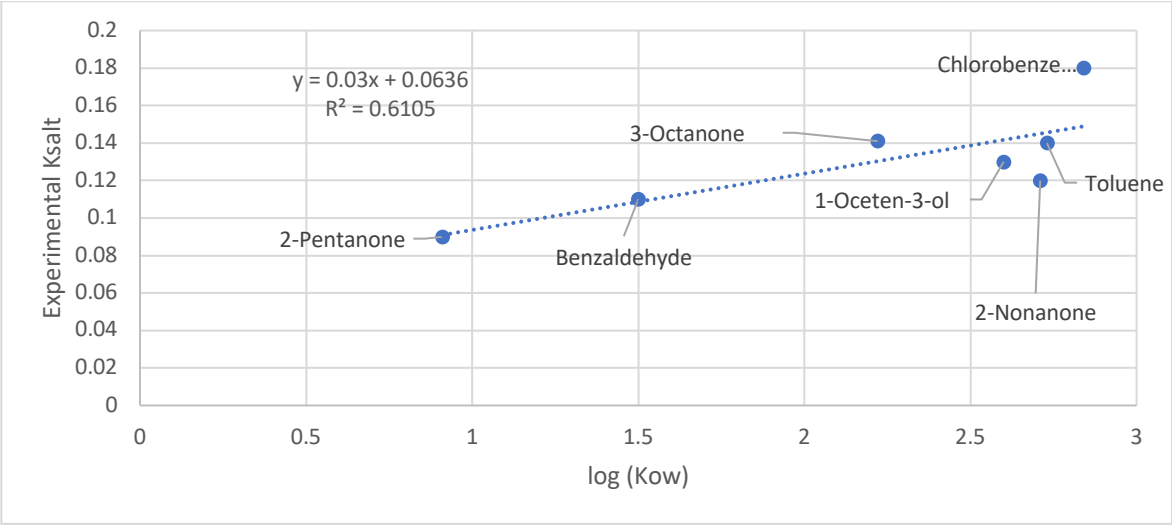

Figure 27. Prediction Curve for any mVOC's K_{MgCl2} based on log(K_{OW}) and experimental K_{MgCl2} for the mVOCs studied. To determine K_{MgCl2} for any mVOC, the equation derived from the curve, $K_{MgCl2} = 0.03log(K_{OW}) + 0.0636$, can be used.

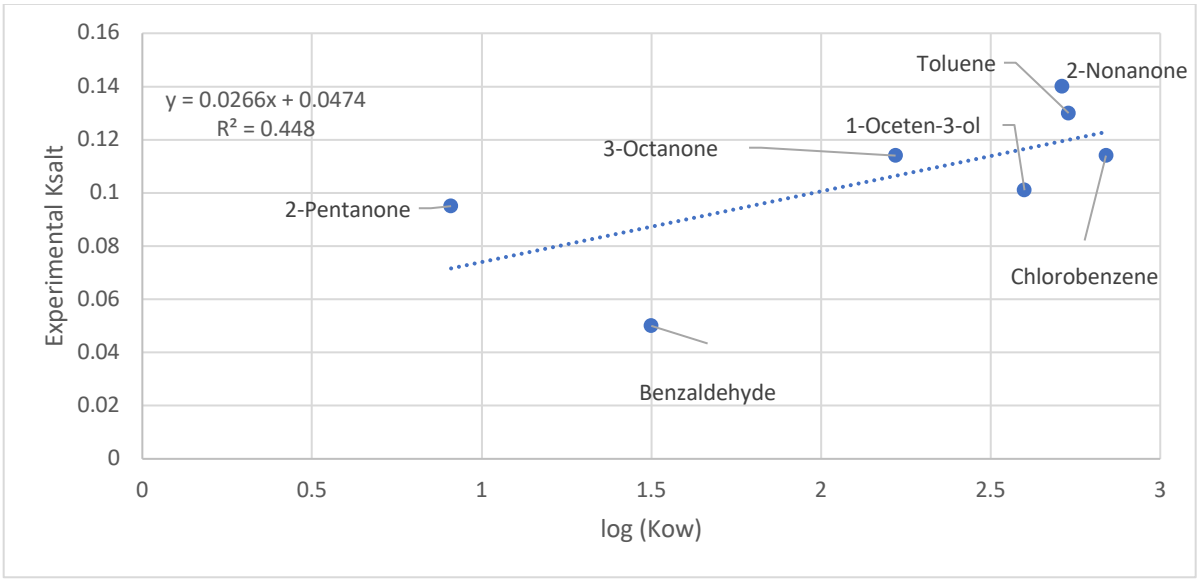

Figure 28. Prediction Curve for any mVOC's K_{NaNO3} based on log(K_{OW}) and experimental K_{NaNO3} for the mVOCs studied. To determine K_{NaNO3} for any mVOC, the equation derived from the curve, $K_{NaNO3} = 0.0266log(K_{OW}) + 0.0474$, can be used.

The following prediction curves (Figures 29-33) were made based on the experimentally obtained KNaCl. The Setschenow coefficients for NaCl are more widely known than other salts, so a prediction model based on the Setschenow coefficient of NaCl of mVOCs can be useful in determining the Setschenow coefficient of other salts. The equations determined were from the linear line of best fit for the seven data points collected for each salt. While the lines are not a perfect fit for the data, they can provide a semi-accurate prediction for mVOCs not yet studied.

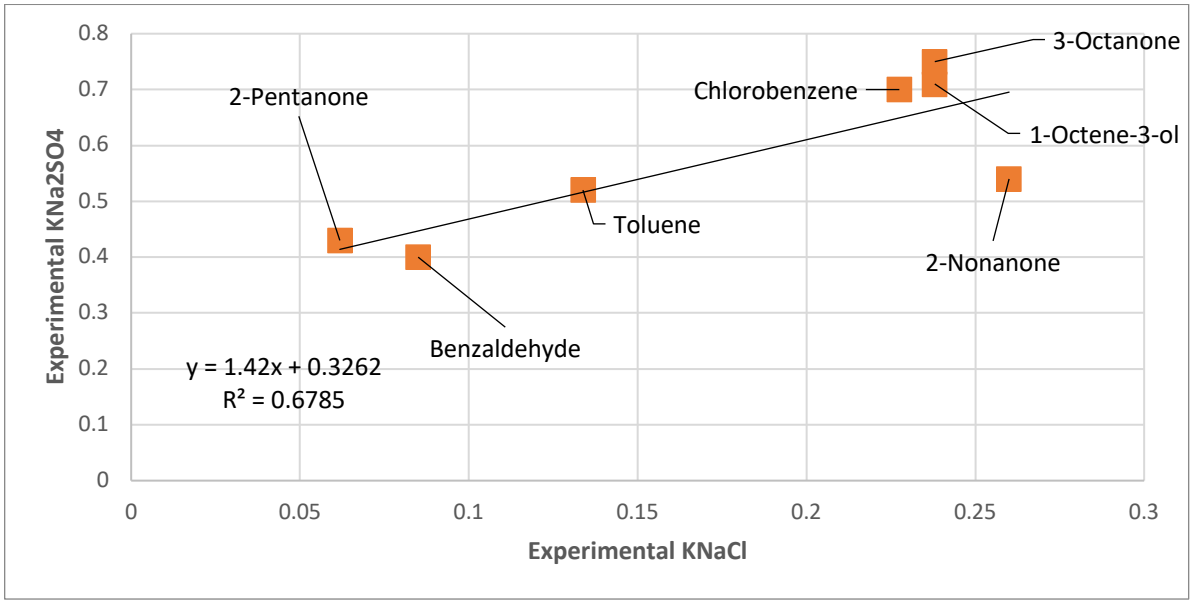

Figure 29. Prediction Curve for K_{Na2SO4} based on experimental K_{Na2SO4} and experimental K_{NaCl} for the mVOCs studied. To determine K_{Na2SO4} for any mVOC, the equation derived from the curve, $K_{Na2SO4} = 1.42K_{NaCl} + 0.3262$, can be used.

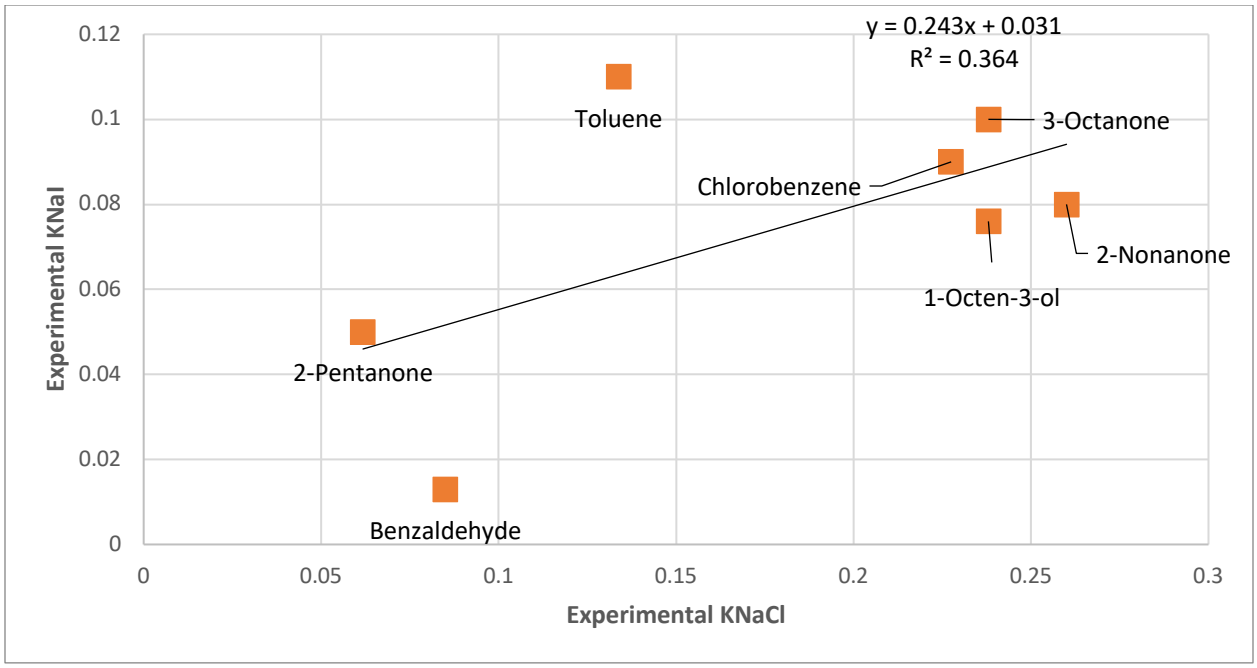

Figure 30. Prediction Curve for K_{NaI} based on experimental K_{Na2SO4} and experimental K_{NaCl} for the mVOCs studied. To determine K_{NaI} for any mVOC, the equation derived from the curve, $K_{NaI} = 0.243K_{NaCl} + 0.031$, can be used.

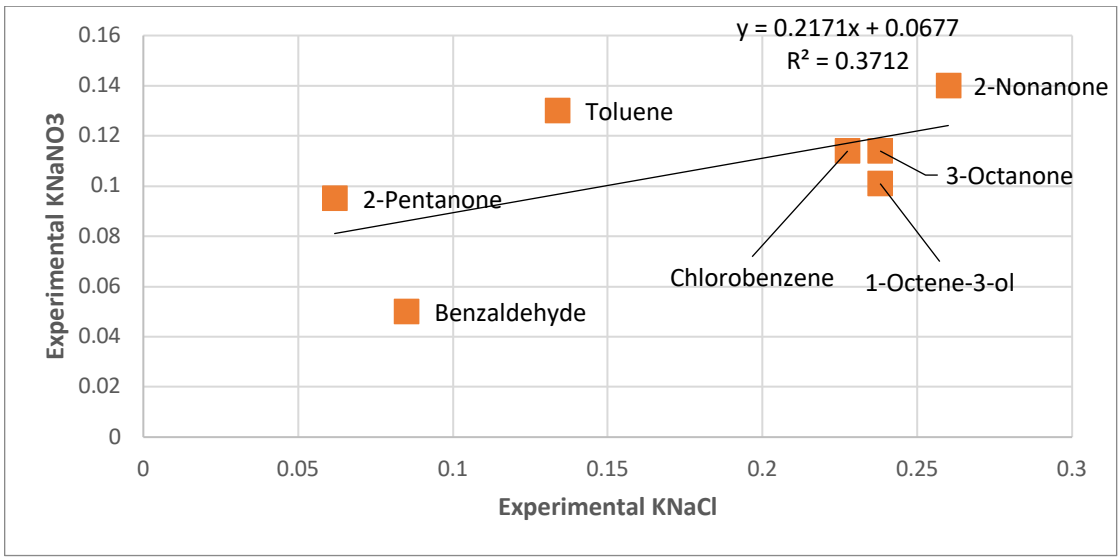

Figure 31. Prediction Curve for K_{NaNO3} based on experimental K_{Na2SO4} and experimental K_{NaCl} for the mVOCs studied. To determine K_{NaNO3} for any mVOC, the equation derived from the curve, $K_{NaNO3} = 0.2171K_{NaCl} + 0.0677$, can be used.

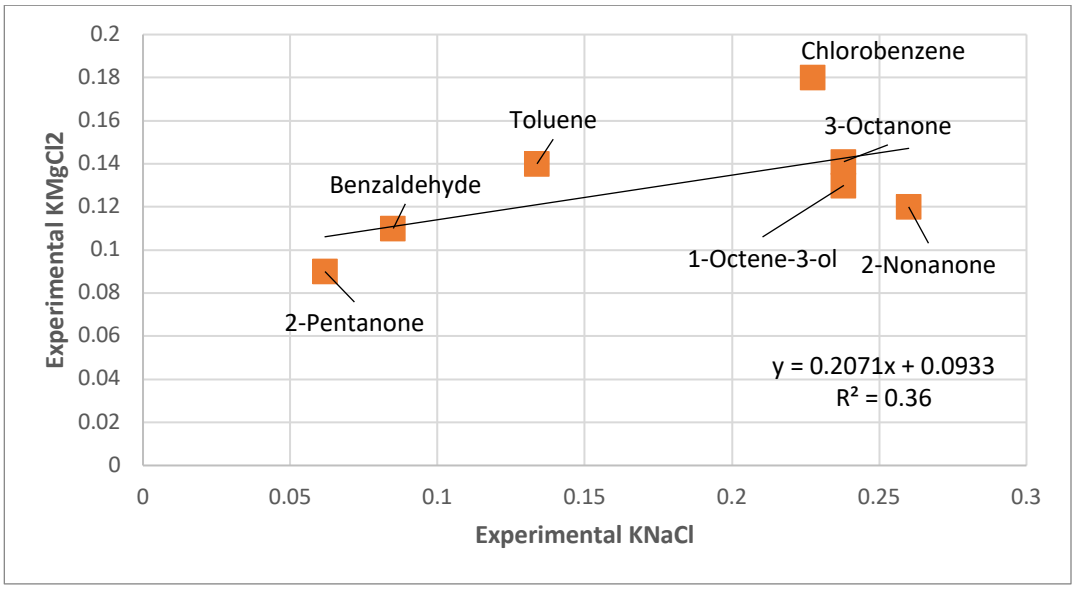

Figure 32. Prediction Curve for K_{MgCl2} based on experimental K_{MgCl2} and experimental K_{NaCl} for the mVOCs studied. To determine K_{MgCl2} for any mVOC, the equation derived from the curve, $K_{MgCl2} = 0.2071K_{NaCl} + 0.0933$, can be used.

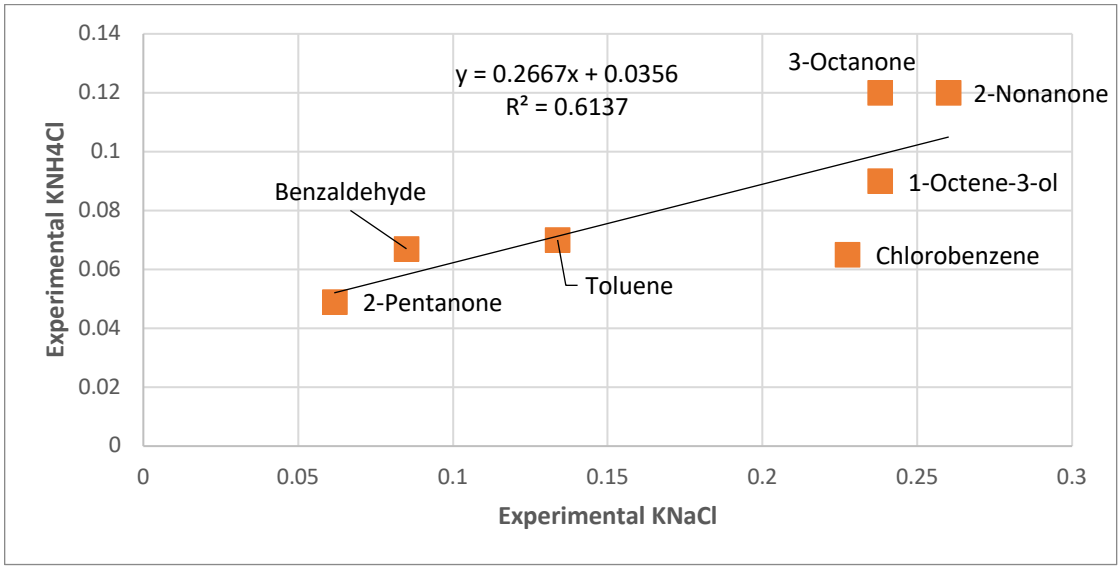

Figure 33. Prediction Curve for K_{NH4Cl} based on experimental K_{NH4Cl} and experimental K_{NaCl} for the mVOCs studied. To determine K_{NH4Cl} for any mVOC, the equation derived from the curve, $K_{NH4Cl} = 0.2667K_{NaCl} + 0.0356$, can be used.

Salt	R^2 of graph based on K_{OW}	R^2 of graph based on K_{NaCl}
Na_2SO_4	0.4069	0.6785
NaCl	0.638	------
$MgCl_2$	0.6105	0.36
$NaNO_3$	0.448	0. 3712
NH_4Cl	0.2278	0. 6137
NaI	0.5379	0.364

Table 16. R^2 values of both methods

To compare the predicative power of the two predictive methods tried, the R^2 values obtained from the graphs (Figures 23-33) were compared in Table 16. There is no value for the R^2 of NaCl based on the K_{NaCl} graph because it will always be 1. The R^2 values are not very close between the two predictive models, with most of them differing by more than 25%. Also, no one method appears to be better than the other. For Na_2SO_4 and NH_4Cl, the prediction using K_{NaCl} is better but overall the R^2 values for these salts were higher (average of 0.6461 for the two salts). For $MgCl_2$, $NaNO_3$, and NaI, the prediction using K_{OW} was better but overall produced lower R^2 values these salts (average of 0.532 for the three salts). Overall, however, the average R^2 value for all the salts across both the K_{OW} and the K_{NaCl} model were virtually the same (0.478 and 0.477, respectively). This means that no one model is better at predicting the Setschenow coefficients than the other.

Conclusions

In conclusion, the salting-out effects of these mVOCs appear to follow the Hofmeister Series for anions (apart from 2-pentanone), but the same is not true for the Hofmeister Series for cations. There could be affects that were not observed in this study (such as polarity) that could cause this discrepancy. Another possible explanation is that there needs to be more trials run for some of the mVOCs to reduce error bars and have more precise data sets. It is known that anions have a more rigid sequence and are less likely to stray from the Hofmeister Series. However, cations are known to be more variable and sensitive to the nature and polarity of the solute[45] which could explain this discrepancy. Further testing can be done to determine the effect of the polarity of the compounds.

With limited data points, it is hard to observe if the predictive models work. The R^2 values for most are very low, but in studies (such as Ni et al[40,41]) that have more datapoints, the R^2 values become higher. This could mean that there is additional work required to determine if these models are accurate, and if one is better than the other. Based on the data available from this experiment, it appears that both methods are about equal in their predictive power. Depending on the salt, one may be better than the other, but there is no correlation between the salts that produce a higher R^2 value for the K_{OW} model or the K_{NaCl} model.

Overall, the data collected in this study could be useful to help predict pathways to human exposure. Building an accurate dataset of Setschenow coefficients is beneficial to accurately predicting how mold, fungi, and other mVOC emitting compounds can affect human health, especially in closed quarters. mVOCs can cause health issues when exposed over long periods of time, and due to humans spending 90% of their time indoors, it is important to know how these mVOCs are being exposed to humans.

References

1. Korpi, A.; Järnberg ‚Jill; and Pasanen, A.-L. Microbial Volatile Organic Compounds. *Critical Reviews in Toxicology* **2009**, *39* (2), 139–193. https://doi.org/10.1080/10408440802291497.
2. Schleibinger, H.; LauBmann, D.; Brattig, C.; Mangler, M.; Eis, D.; Ruden, H. Emission Patterns and Emission Rates of MVOC and the Possibility for Predicting Hidden Mold Damage? *Indoor Air* **2005**, *15*, 98–104. https://doi.org/10.1111/j.1600-0668.2005.00349.x.
3. *mVOC 4.0*. mVOC 4.0. https://bioinformatics.charite.de/mvoc/index.php?site=ergebnis.
4. Tabbal, S.; El Aroussi, B.; Bouchard, M.; Marchand, G.; Haddad, S. Development and Validation of a Method for the Simultaneous Quantification of 21 Microbial Volatile Organic Compounds in Ambient and Exhaled Air by Thermal Desorption and Gas Chromatography–Mass Spectrometry. *Atmosphere* **2022**, *13* (1432). https://doi.org/https://doi.org/10.3390/atmos13091432.
5. Li, L.; Arnot, J. A.; Wania, F. How Are Humans Exposed to Organic Chemicals Released to Indoor Air? *Environ. Sci. Technol.* **2019**, *53* (19), 11276–11284. https://doi.org/10.1021/acs.est.9b02036.
6. Wu, S.; Hayati, S. K.; Kim, E.; De La Mata, A. P.; Harynuk, J. J.; Wang, C.; Zhao, R. Henry's Law Constants and Indoor Partitioning of Microbial Volatile Organic Compounds. *Environ. Sci. Technol.* **2022**, *56* (11), 7143–7152. https://doi.org/10.1021/acs.est.1c07882.
7. Wazeerud-Din, I. J.; Silva, L. K.; Smith, M. M.; Newman, C. A.; Blount, B. C.; De Jesús, V. R. Quantification of Seven Microbial Volatile Organic Compounds in Human Serum by Solid-Phase Microextraction Gas Chromatography-Tandem Mass Spectrometry. *Chemosphere* **2021**, *266*, 128970. https://doi.org/10.1016/j.chemosphere.2020.128970

8. Sahlberg, B.; Gunnbjörnsdottir, M.; Soon, A.; Jogi, R.; Gislason, T.; Wieslander, G.; Janson, C.; Norback, D. Airborne Molds and Bacteria, Microbial Volatile Organic Compounds (MVOC), Plasticizers and Formaldehyde in Dwellings in Three North European Cities in Relation to Sick Building Syndrome (SBS). *Science of The Total Environment* **2013**, *444*, 433–440. https://doi.org/10.1016/j.scitotenv.2012.10.114.
9. Garcia-Alcega, S.; Nasir, Z. A.; Ferguson, R.; Whitby, C.; Dumbrell, A. J.; Colbeck, I.; Gomes, D.; Tyrrel, S.; Coulon, F. Fingerprinting Outdoor Air Environment Using Microbial Volatile Organic Compounds (MVOCs) – A Review. *TrAC Trends in Analytical Chemistry* **2017**, *86*, 75–83. https://doi.org/10.1016/j.trac.2016.10.010.
10. Kalalian, C.; Abis, L.; Depoorter, A.; Lunardelli, B.; Perrier, S.; George, C. Influence of Indoor Chemistry on the Emission of MVOCs from Aspergillus Niger Molds. *Science of The Total Environment* **2020**, *741*, 140148. https://doi.org/10.1016/j.scitotenv.2020.140148.
11. Vesper, S.; Barnes, C.; Ciaccio, C. E.; Johanns, A.; Kennedy, K.; Murphy, J. S.; Nunez-Alvarez, A.; Sandel, M. T.; Cox, D.; Dewalt, G.; Ashley, P. J. Higher Environmental Relative Moldiness Index (ERMI) Values Measured in Homes of Asthmatic Children in Boston, Kansas City, and San Diego. *Journal of Asthma* **2013**, *50* (2), 155–161. https://doi.org/10.3109/02770903.2012.740122.
12. Fiedler, K.; Schütz, E.; Geh, S. Detection of Microbial Volatile Organic Compounds (MVOCs) Produced by Moulds on Various Materials. *International Journal of Hygiene and Environmental Health* **2001**, *204* (2), 111–121. https://doi.org/10.1078/1438-4639-00094.
13. Blanc, P. D.; Quinlan, P. J.; Katz, P. P.; Balmes, J. R.; Trupin, L.; Cisternas, M. G.; Wymer, L.; Vesper, S. J. Higher Environmental Relative Moldiness Index Values Measured in Homes

of Adults with Asthma, Rhinitis, or Both Conditions. *Environmental Research* **2013**, *122*, 98–101. https://doi.org/10.1016/j.envres.2013.01.002.

14. Matysik, S.; Herbarth, O.; Mueller, A. Determination of Volatile Metabolites Originating from Mould Growth on Wall Paper and Synthetic Media. *Journal of Microbiological Methods* **2008**, *75* (2), 182–187. https://doi.org/10.1016/j.mimet.2008.05.027.
15. Araki, A.; Ketema, R. M.; Ait Bamai, Y.; Kishi, R. Aldehydes, Volatile Organic Compounds (VOCs), and Health. In *Indoor Environmental Quality and Health Risk toward Healthier Environment for All*; Kishi, R., Norbäck, D., Araki, A., Eds.; Springer: Singapore, 2020; pp 129–158. https://doi.org/10.1007/978-981-32-9182-9_7.
16. Zhao, G.; Yin, G.; Inamdar, A. A.; Luo, J.; Zhang, N.; Yang, I.; Buckley, B.; Bennett, J. W. Volatile Organic Compounds Emitted by Filamentous Fungi Isolated from Flooded Homes after Hurricane Sandy Show Toxicity in a Drosophila Bioassay. *Indoor Air* **2017**, *27* (3), 518–528. https://doi.org/10.1111/ina.12350.
17. Kjærgaard, S. K.; Mølhave, L.; Pedersen, O. F. Human Reactions to a Mixture of Indoor Air Volatile Organic Compounds. *Atmospheric Environment. Part A. General Topics* **1991**, *25* (8), 1417–1426. https://doi.org/10.1016/0960-1686(91)90001-N.
18. Korpi, A.; Kasanen ,Jukka-Pekka; Alarie ,Yves; Kosma ,Veli-Matti; and Pasanen, A.-L. Sensory Irritating Potency of Some Microbial Volatile Organic Compounds (MVOCs) and a Mixture of Five MVOCs. *Archives of Environmental Health: An International Journal* **1999**, *54* (5), 347–352. https://doi.org/10.1080/00039899909602499.
19. Inamdar, A. A.; Hossain, M. M.; Bernstein, A. I.; Miller, G. W.; Richardson, J. R.; Bennett, J. W. Fungal-Derived Semiochemical 1-Octen-3-Ol Disrupts Dopamine Packaging and

Causes Neurodegeneration. *Proc. Natl. Acad. Sci. U.S.A.* **2013**, *110* (48), 19561–19566. https://doi.org/10.1073/pnas.1318830110.

20. Wålinder, R.; Ernstgård, L.; Norbäck, D.; Wieslander, G.; Johanson, G. Acute Effects of 1-Octen-3-Ol, a Microbial Volatile Organic Compound (MVOC)--an Experimental Study. *Toxicol Lett* **2008**, *181* (3), 141–147. https://doi.org/10.1016/j.toxlet.2008.07.013.
21. Smith, F.; Harvey, A. *Environmental Management*. https://tsapps.nist.gov/publication/get_pdf.cfm?pub_id=50449.
22. Meylan, W. M.; Howard, P. H. Estimating Octanol–Air Partition Coefficients with Octanol–Water Partition Coefficients and Henry's Law Constants. *Chemosphere* **2005**, *61* (5), 640–644. https://doi.org/10.1016/j.chemosphere.2005.03.029.
23. Avishay, D. M.; Tenny, K. M. Henry's Law. In *StatPearls [Internet]*; StatPearls Publishing, 2023.
24. Staudinger, J.; and Roberts, P. V. A Critical Review of Henry's Law Constants for Environmental Applications. *Critical Reviews in Environmental Science and Technology* **1996**, *26* (3), 205–297. https://doi.org/10.1080/10643389609388492.
25. Sander, R. Compilation of Henry's Law Constants (Version 4.0) for Water as Solvent. *Atmospheric Chemistry and Physics* **2015**, *15* (8), 4399–4981. https://doi.org/10.5194/acp-15-4399-2015.
26. Huerta-Diaz, M. A.; Rodriguez, S. Solubility Measurements and Determination of Setschenow Constants for the Pesticide Carbaryl in Seawater and Other Electrolyte Solutions. *Can. J. Chem.* **1992**, *70* (12), 2864–2868. https://doi.org/10.1139/v92-365.
27. Xu, J.; Wang, L.; Wang, L.; Liang, G.; Shen, X.; Xu, W. Prediction of Setschenow Constants of Organic Compounds Based on a 3D Structure Representation. *Chemometrics and*

Intelligent Laboratory Systems **2011**, *107* (1), 178–184. https://doi.org/10.1016/j.chemolab.2011.03.006.

28. Waxman, E. M.; Elm, J.; Kurtén, T.; Mikkelsen, K. V.; Ziemann, P. J.; Volkamer, R. Glyoxal and Methylglyoxal Setschenow Salting Constants in Sulfate, Nitrate, and Chloride Solutions: Measurements and Gibbs Energies. *Environ. Sci. Technol.* **2015**, *49* (19), 11500–11508. https://doi.org/10.1021/acs.est.5b02782.
29. De Stefano, C.; Lando, G.; Malegori, C.; Oliveri, P.; Sammartano, S. Prediction of Water Solubility and Setschenow Coefficients by Tree-Based Regression Strategies. *Journal of Molecular Liquids* **2019**, *282*, 401–406. https://doi.org/10.1016/j.molliq.2019.03.029.
30. Xie, W.-H.; Shiu, W.-Y.; Mackay, D. A Review of the Effect of Salts on the Solubility of Organic Compounds in Seawater. *Marine Environmental Research* **1997**, *44* (4), 429–444. https://doi.org/10.1016/S0141-1136(97)00017-2.
31. Sergeeva, V. SALTING-OUT AND SALTING-IN OF NONELECTROLYTES. *Russian Chemical Reviews* **1965**, *34* (4), 309–318.
32. Jonker, M. T. O.; Muijs, B. Using Solid Phase Micro Extraction to Determine Salting-out (Setschenow) Constants for Hydrophobic Organic Chemicals. *Chemosphere* **2010**, *80* (3), 223–227. https://doi.org/10.1016/j.chemosphere.2010.04.041.
33. Bretti, C.; Cigala, R. M.; De Stefano, C.; Lando, G.; Sammartano, S. Survey of the Solubility Data of Organic Molecules. Classification and Modeling of the Factors Influencing Setschenow Coefficients in Several Ionic Media; ITA, 2017.
34. Valderrama, J. O.; Campusano, R. A.; Forero, L. A. A New Generalized Henry-Setschenow Equation for Predicting the Solubility of Air Gases (Oxygen, Nitrogen and Argon) in

Seawater and Saline Solutions. *Journal of Molecular Liquids* **2016**, *222*, 1218–1227. https://doi.org/10.1016/j.molliq.2016.07.110.

35. ZHANG, Y.; CREMER, P. Interactions between Macromolecules and Ions: The Hofmeister Series. *Current Opinion in Chemical Biology* **2006**, *10* (6), 658–663. https://doi.org/10.1016/j.cbpa.2006.09.020.
36. Gregory, K. P.; Elliott, G. R.; Robertson, H.; Kumar, A.; Wanless, E. J.; Webber, G. B.; Craig, V. S. J.; Andersson, G. G.; Page, A. J. Understanding Specific Ion Effects and the Hofmeister Series. *Physical Chemistry Chemical Physics* **2022**, *24* (21), 12682–12718. https://doi.org/10.1039/d2cp00847e.
37. Kang, B.; Tang, H.; Zhao, Z.; Song, S. Hofmeister Series: Insights of Ion Specificity from Amphiphilic Assembly and Interface Property. *ACS Omega* **2020**, *5* (12), 6229–6239. https://doi.org/10.1021/acsomega.0c00237.
38. Thet, K.; Woo, N. *Gas Chromatography*. Chemistry LibreTexts. https://chem.libretexts.org/Bookshelves/Analytical_Chemistry/Supplemental_Modules_(Analytical_Chemistry)/Instrumentation_and_Analysis/Chromatography/Gas_Chromatography.
39. Yu, X.; Yu, R. Setschenow Constant Prediction Based on the IEF-PCM Calculations. *Ind. Eng. Chem. Res.* **2013**, *52* (32), 11182–11188. https://doi.org/10.1021/ie400001u.
40. Ni, N.; Yalkowsky, S. H. Prediction of Setschenow Constants. *International Journal of Pharmaceutics* **2003**, *254* (2), 167–172. https://doi.org/10.1016/S0378-5173(03)00008-5.
41. Burant, A.; Lowry, G. V.; Karamalidis, A. K. Measurement and Modeling of Setschenow Constants for Selected Hydrophilic Compounds in NaCl and CaCl2 Simulated Carbon Storage Brines. *Acc. Chem. Res.* **2017**, *50* (6), 1332–1341. https://doi.org/10.1021/acs.accounts.6b00567.

42. Burant, A.; Lowry, G. V.; Karamalidis, A. K. Measurement of Setschenow Constants for Six Hydrophobic Compounds in Simulated Brines and Use in Predictive Modeling for Oil and Gas Systems. *Chemosphere* **2016**, *144*, 2247–2256. https://doi.org/10.1016/j.chemosphere.2015.10.115.

43. Ni, N.; El-Sayed, M. M.; Sanghvi, T.; Yalkowsky, S. H. Estimation of the Effect of NaCl on the Solubility of Organic Compounds in Aqueous Solutions. *J Pharm Sci* **2000**, *89* (12), 1620–1625. https://doi.org/10.1002/1520-6017(200012)89:12<1620::aid-jps13>3.0.co;2-n.

44. Harris, D. C. Nonlinear Least-Squares Curve Fitting with Microsoft Excel Solver. *J. Chem. Educ.* **1998**, *75* (1), 119. https://doi.org/10.1021/ed075p119.

45. Hyde, A. M.; Zultanski, S. L.; Waldman, J. H.; Zhong, Y.-L.; Shevlin, M.; Peng, F. General Principles and Strategies for Salting-out Informed by the Hofmeister Series. *Organic Process Research & Development* **2017**, *21* (9), 1355–1370. https://doi.org/10.1021/acs.oprd.7b00197.

Appendix Table of Contents

Appendix

Toluene

For all graphs, A is equivalent to $\frac{S_c}{S}$.

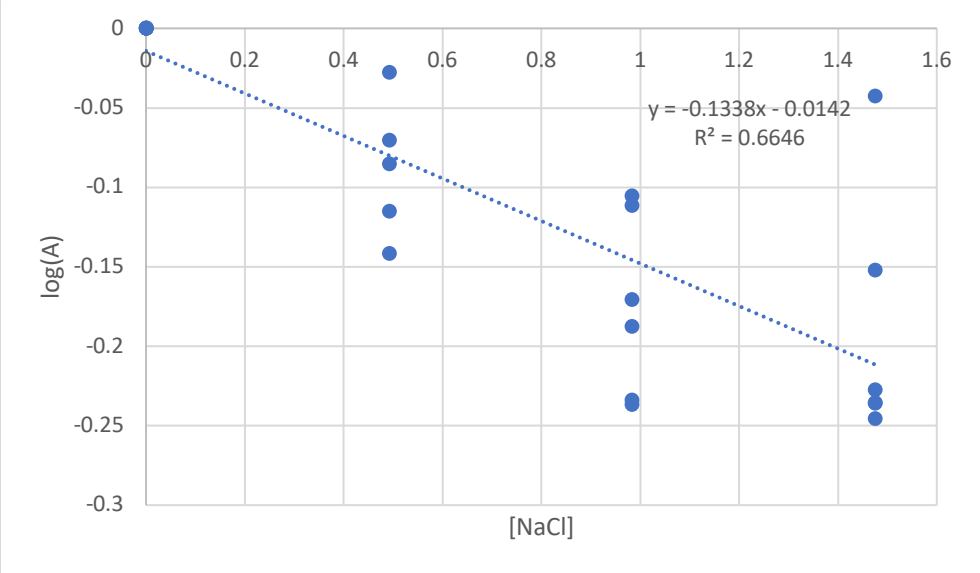

Figure 34. log(A) vs. [NaCl] for toluene.

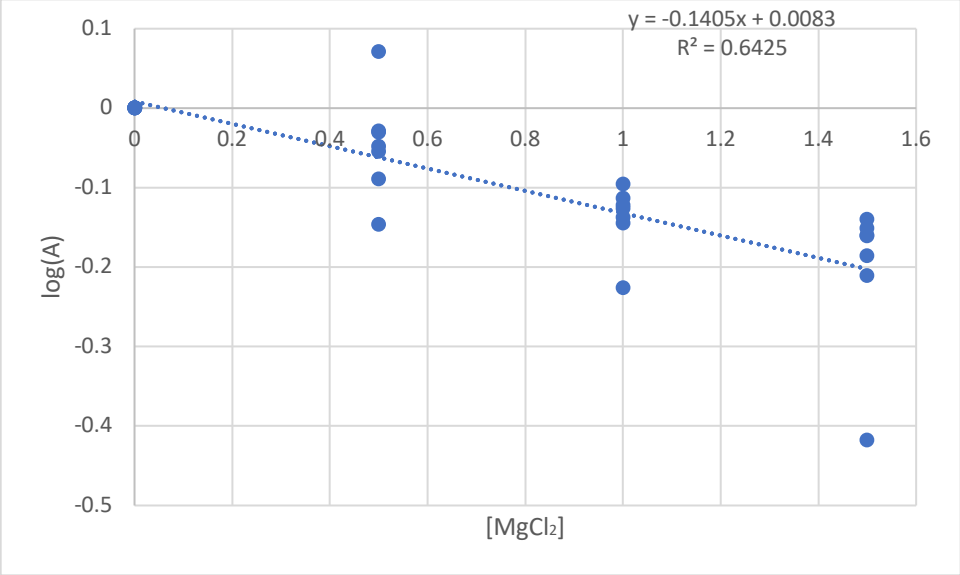

Figure 35. log(A) vs. [$MgCl_2$] for toluene.

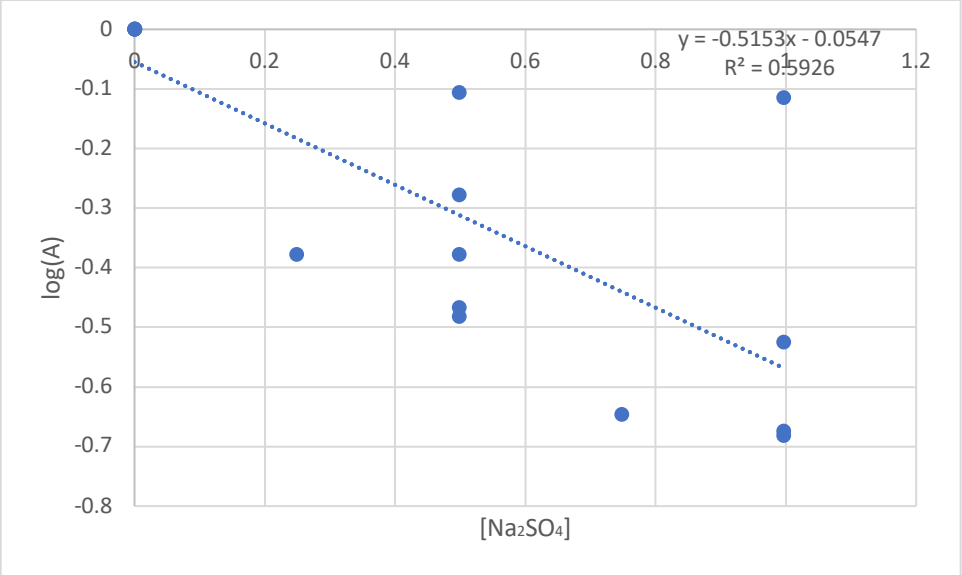

Figure 36. log(A) vs. [Na_2SO_4] for toluene.

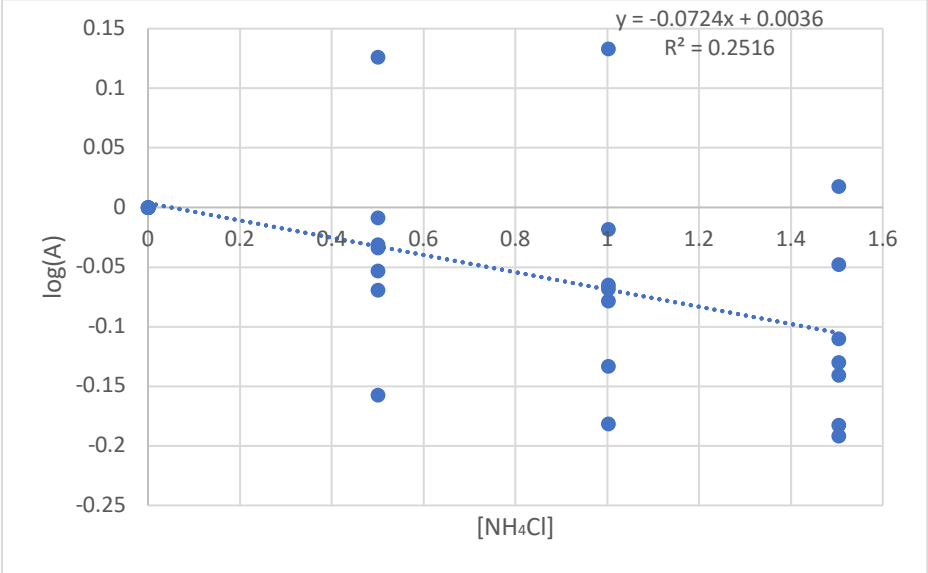

Figure 37. log(A) vs. [NH_4Cl] for toluene.

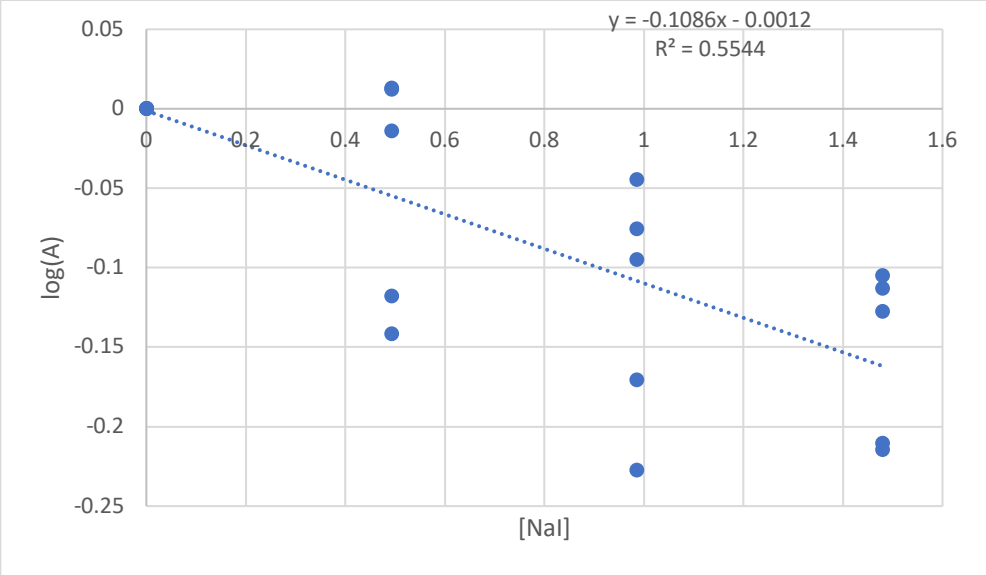

Figure 38. log(A) vs. [NaI] for toluene.

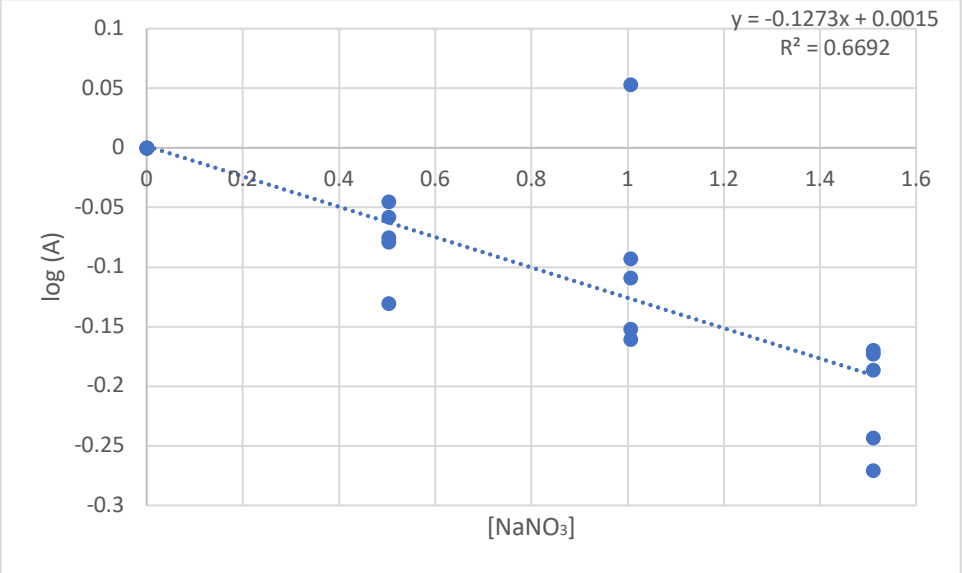

Figure 39. log(A) vs. [$NaNO_3$] for toluene.

3-Octanone

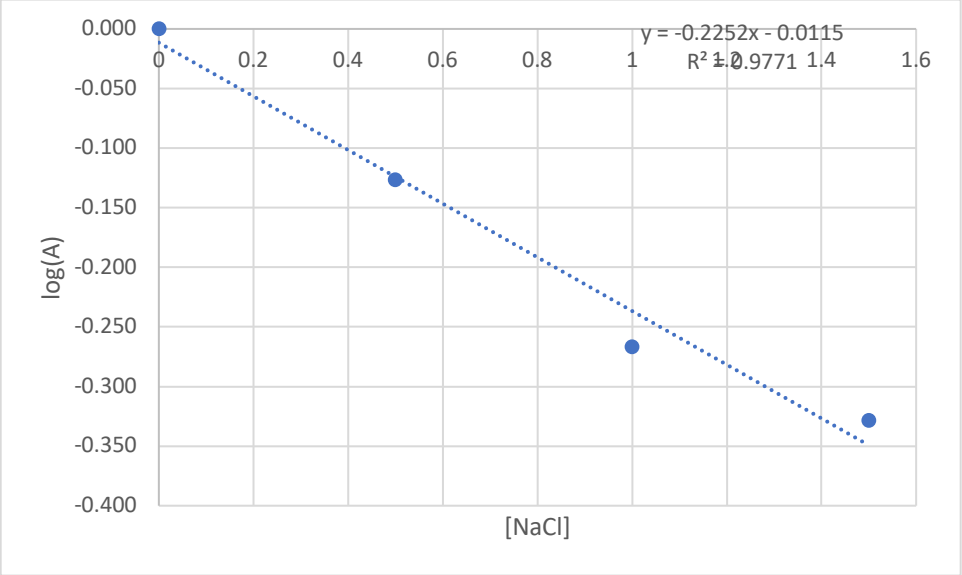

Figure 40. log(A) vs. [NaCl] for 3-octanone.

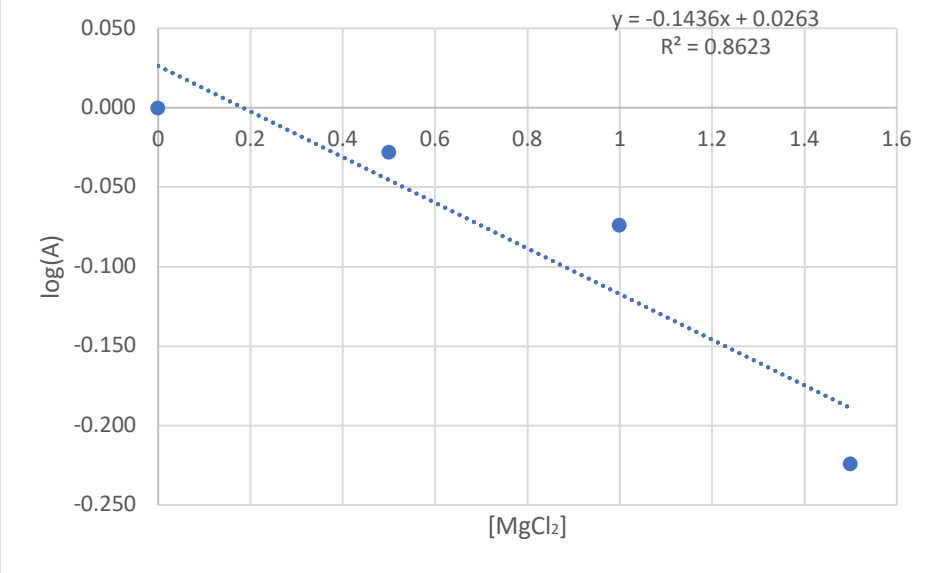

Figure 41. log(A) vs. [$MgCl_2$] for 3-octanone.

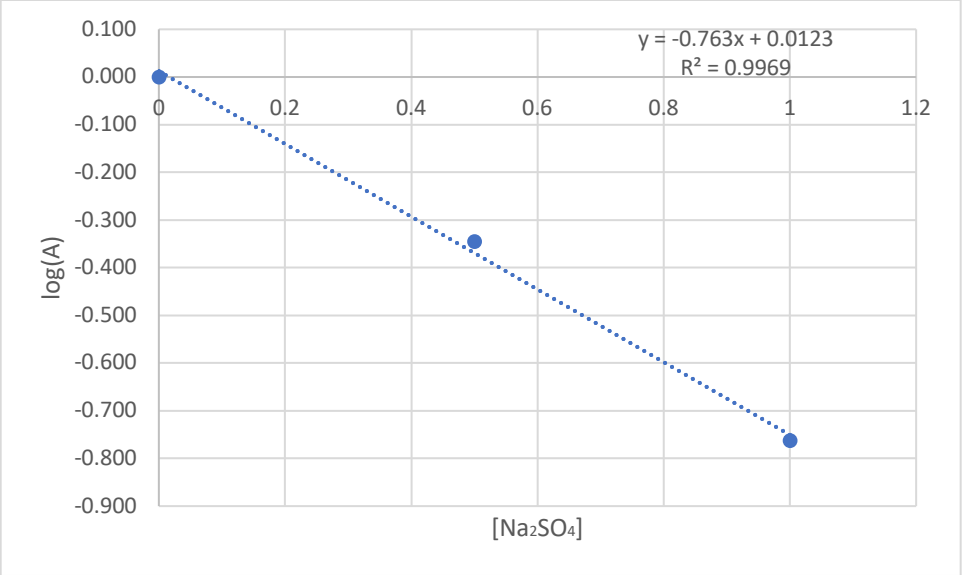

Figure 42. log(A) vs. [Na_2SO_4] for 3-octanone.

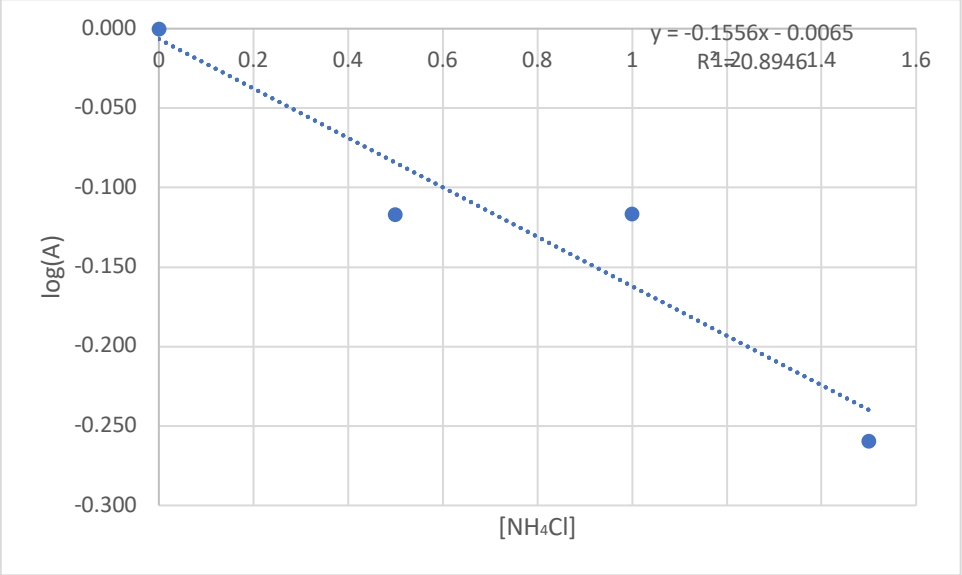

Figure 43. log(A) vs. [NH_4Cl] for 3-octanone.

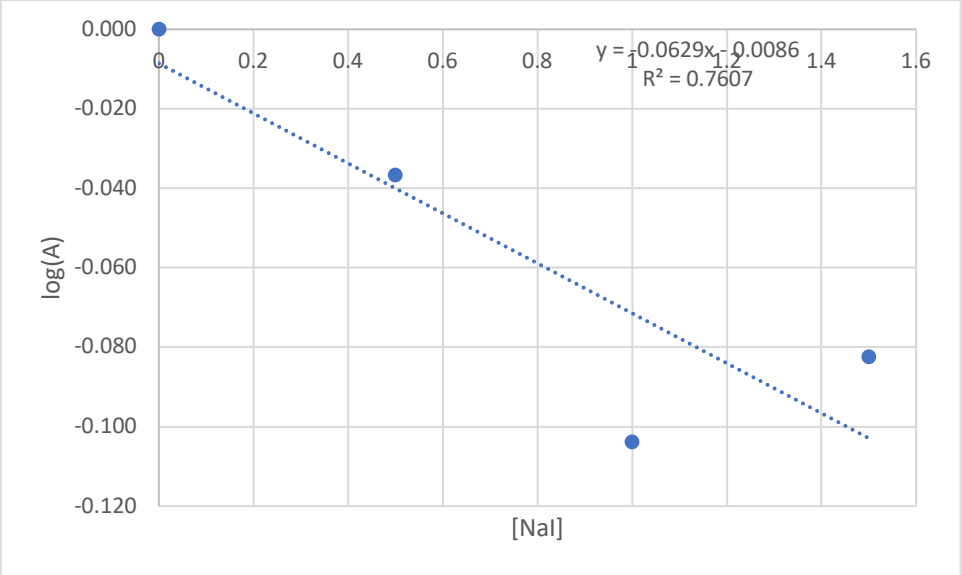

Figure 44. log(A) vs. [NaI] for 3-octanone.

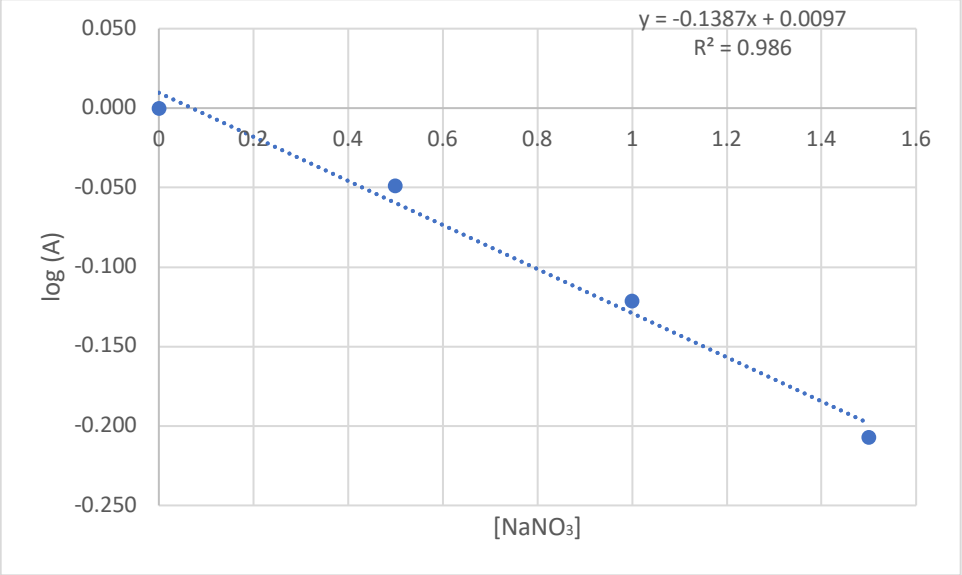

Figure 45. log(A) vs. [$NaNO_3$] for 3-octanone.

1-Octe-3-ol

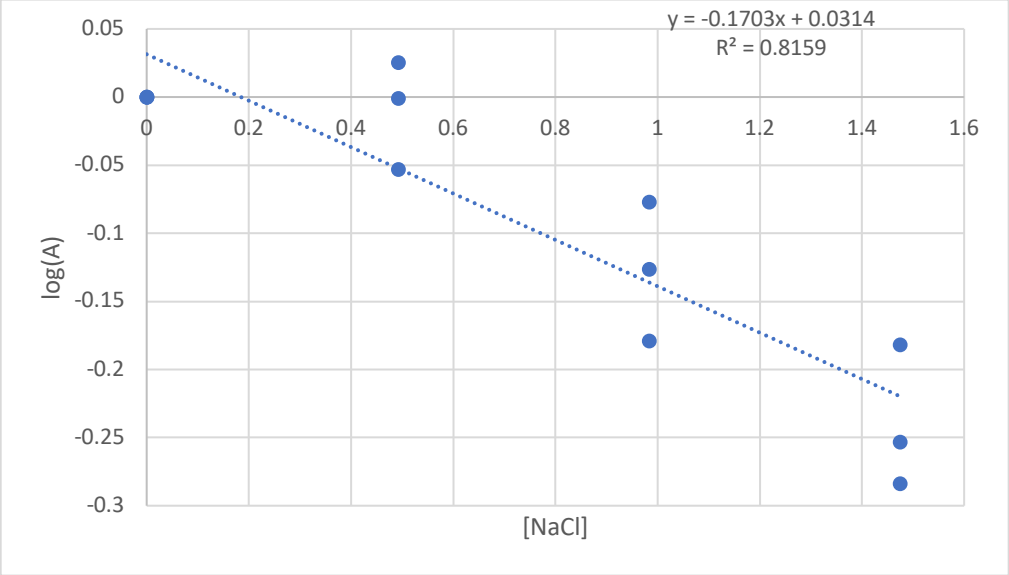

Figure 46. log(A) vs. [NaCl] for 1-octe-3-ol.

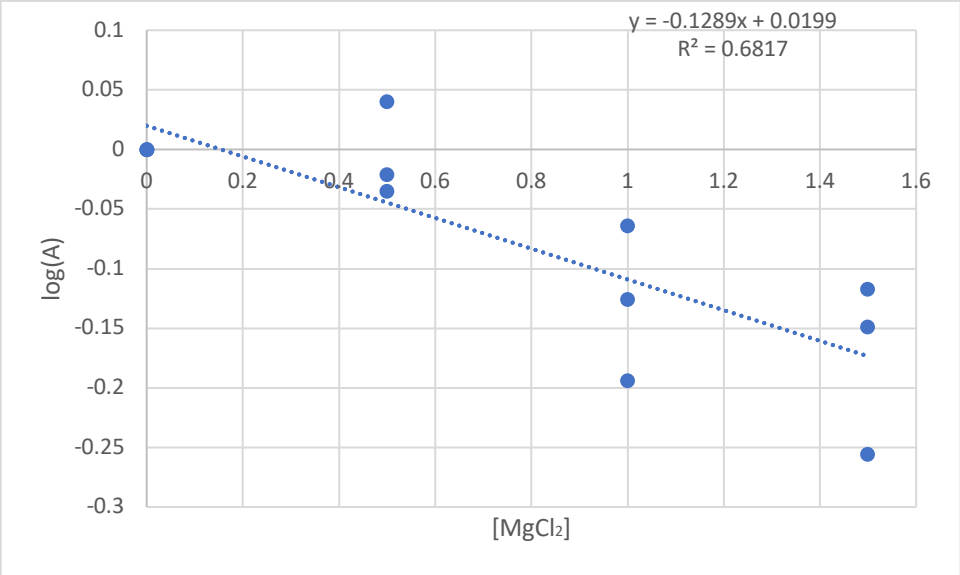

Figure 47. log(A) vs. [$MgCl_2$] for 1-octe-3-ol.

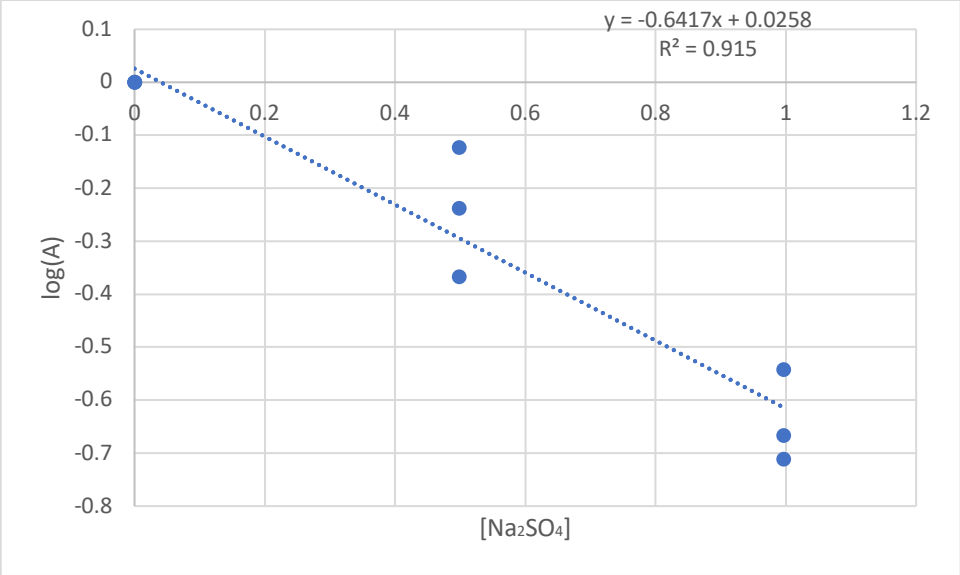

Figure 48. log(A) vs. [Na_2SO_4] for 1-octe-3-ol.

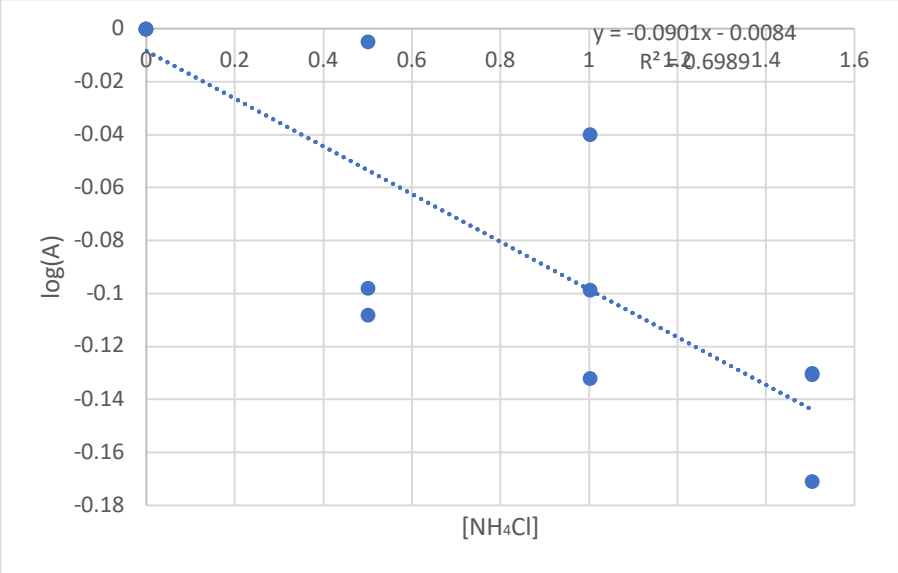

Figure 49. log(A) vs. [NH_4Cl] for 1-octe-3-ol.

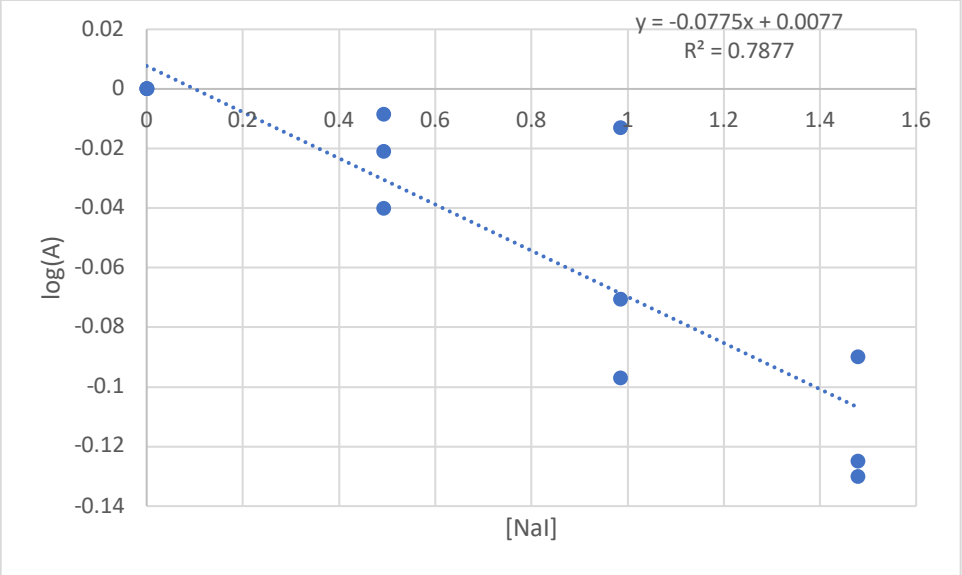

Figure 50. log(A) vs. [NaI] for 1-octe-3-ol.

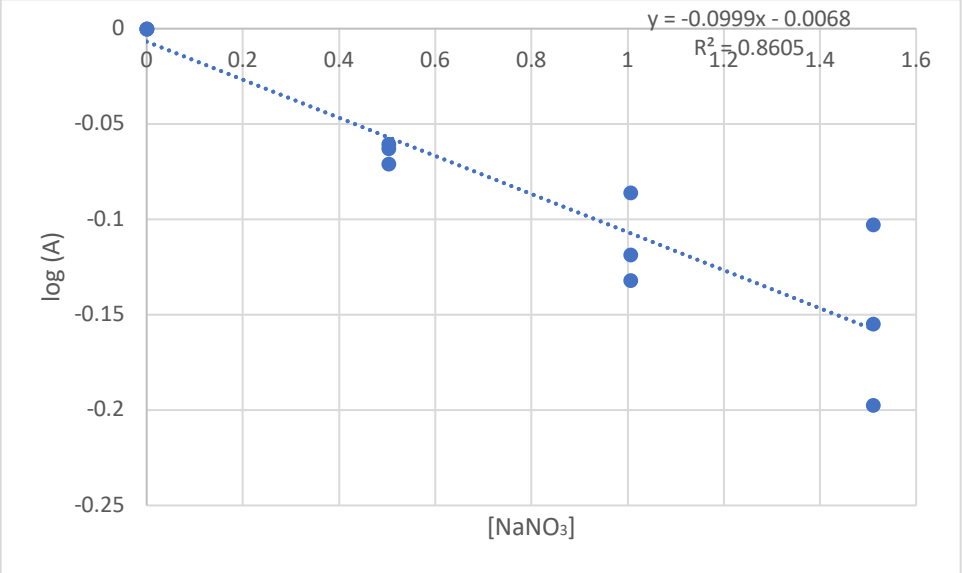

Figure 51. log(A) vs. [$NaNO_3$] for 1-octe-3-ol.

2-Nonanone

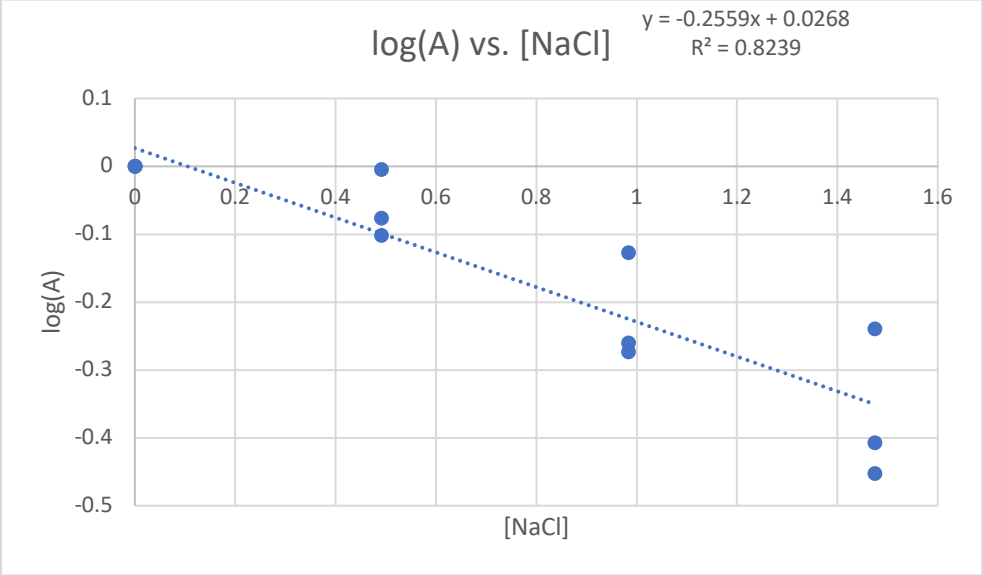

Figure 52. log(A) vs. [NaCl] for 2-nonanone.

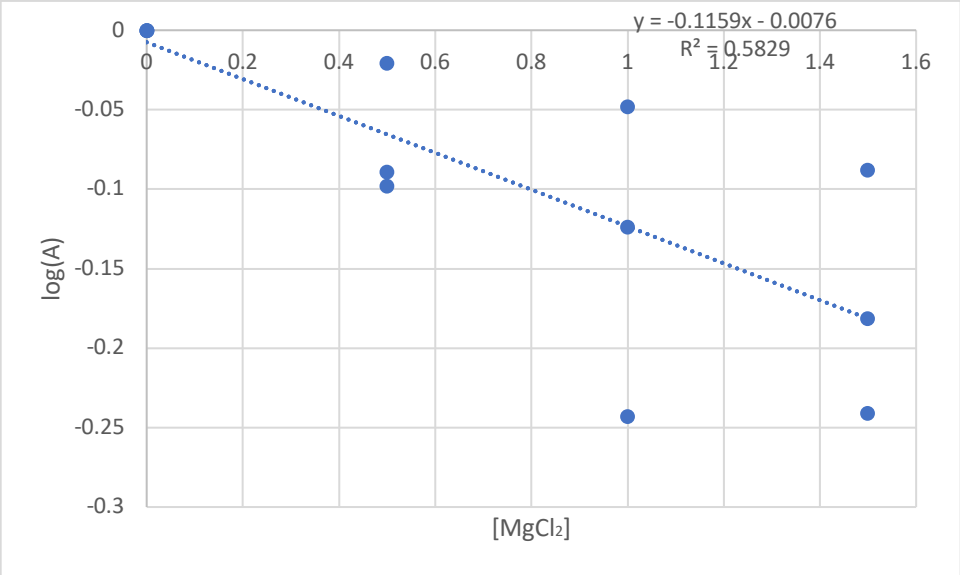

Figure 53. log(A) vs. [$MgCl_2$] for 2-nonanone.

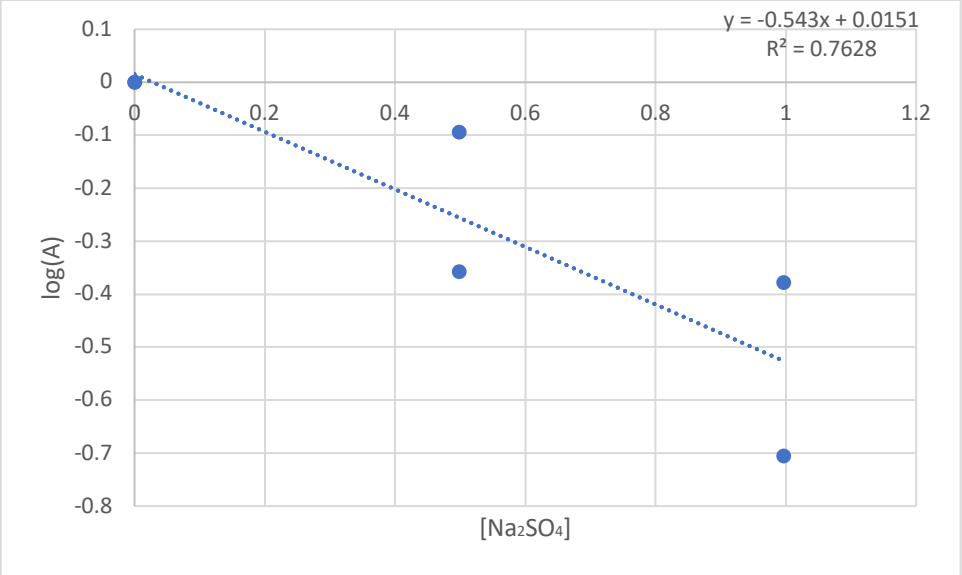

Figure 54. log(A) vs. [Na_2SO_4] for 2-nonanone.

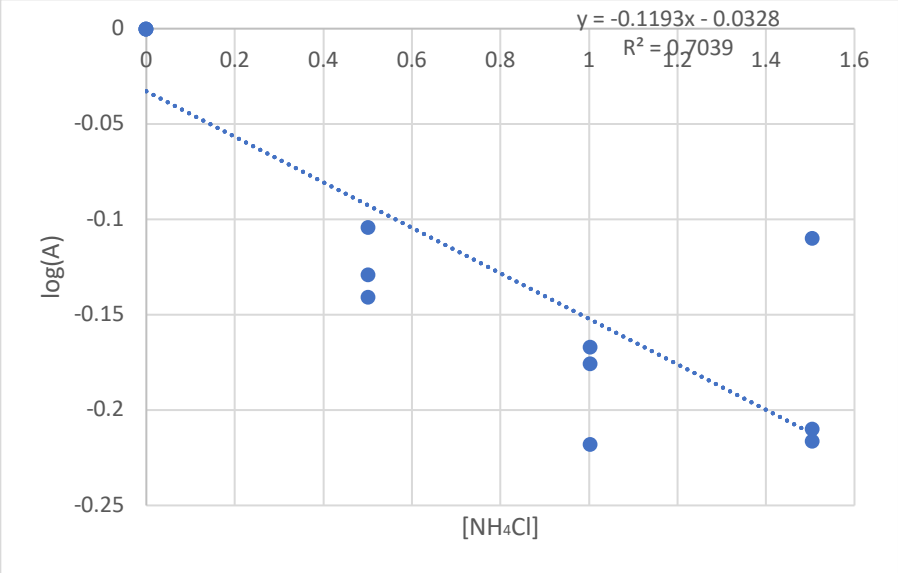

Figure 55. log(A) vs. [NH_4Cl] for 2-nonanone.

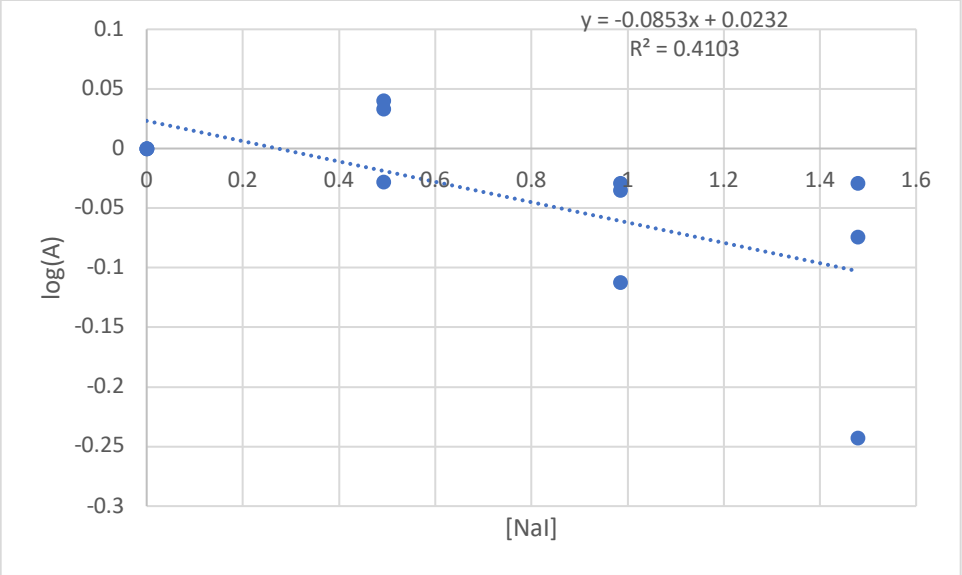

Figure 56. log(A) vs. [NaI] for 2-nonanone.

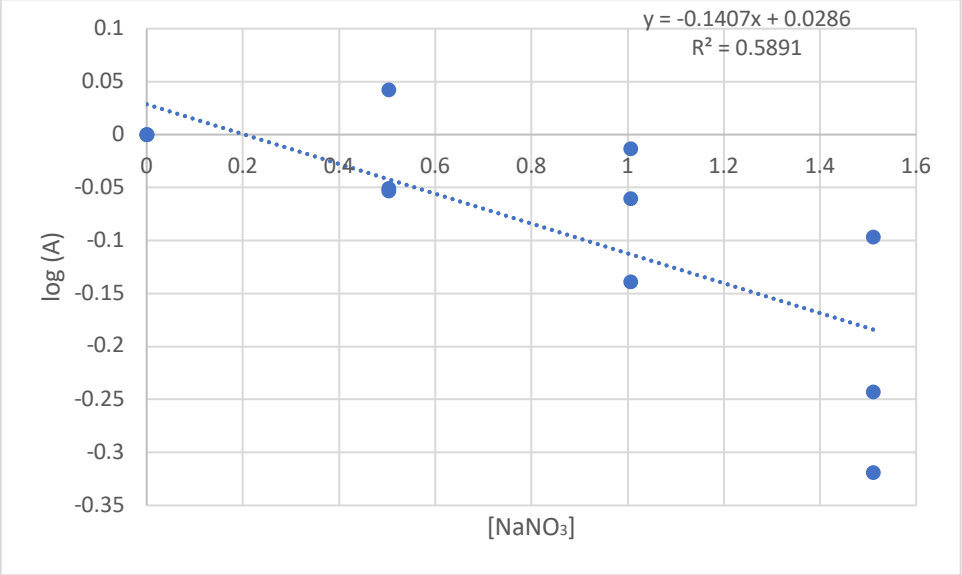

Figure 57. log(A) vs. [$NaNO_3$] for 2-nonanone.

2-Pentanone

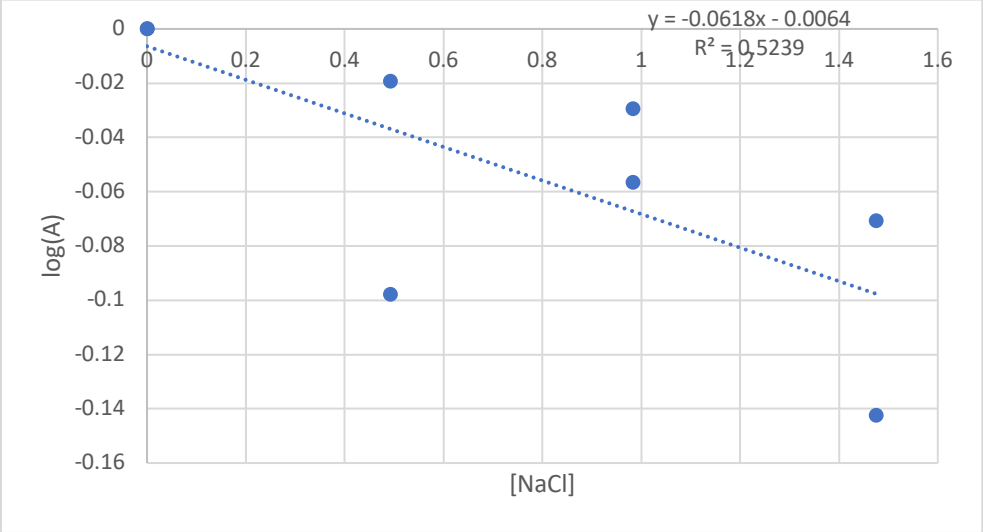

Figure 58. log(A) vs. [NaCl] for 2-pentanone.

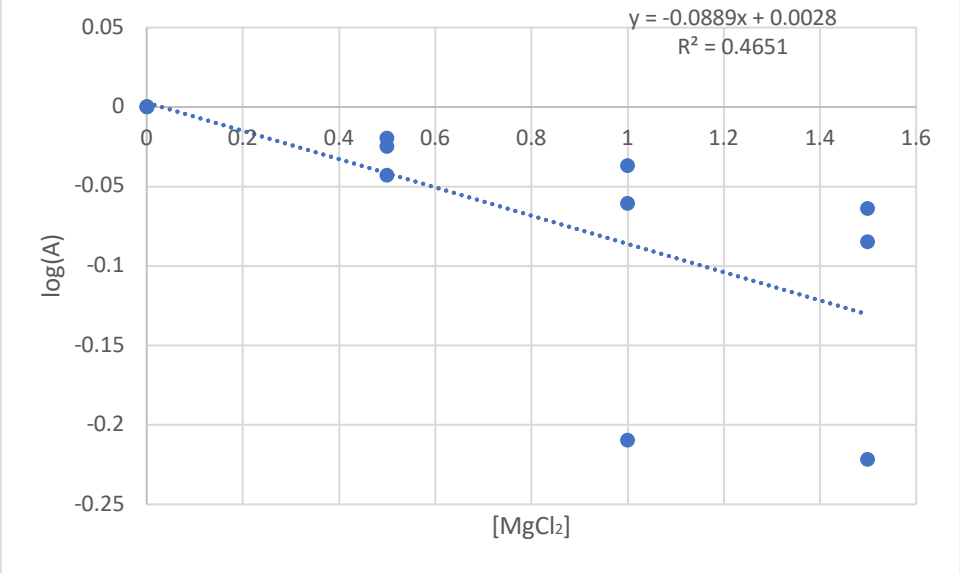

Figure 59. log(A) vs. [$MgCl_2$] for 2-pentanone.

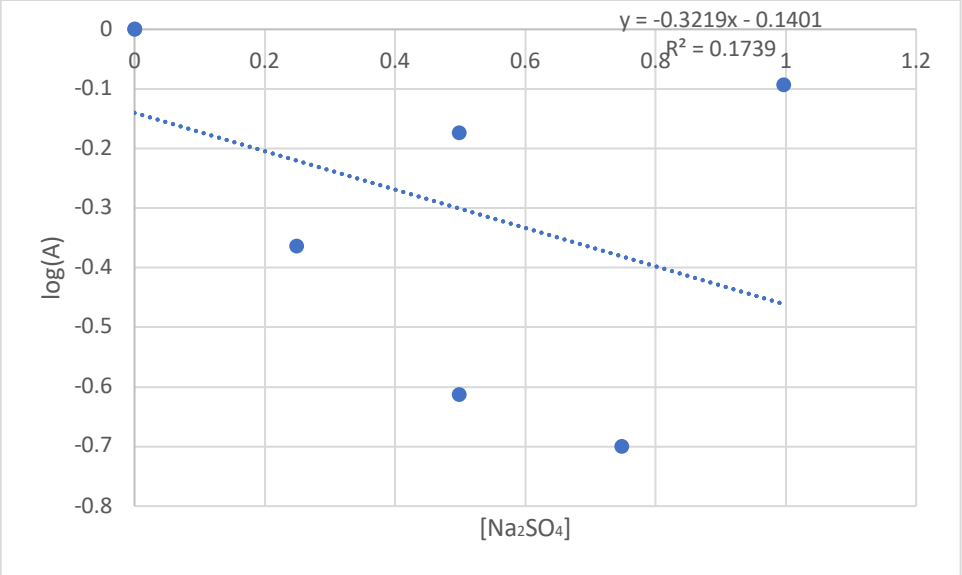

Figure 60. log(A) vs. [Na_2SO_4] for 2-pentanone.

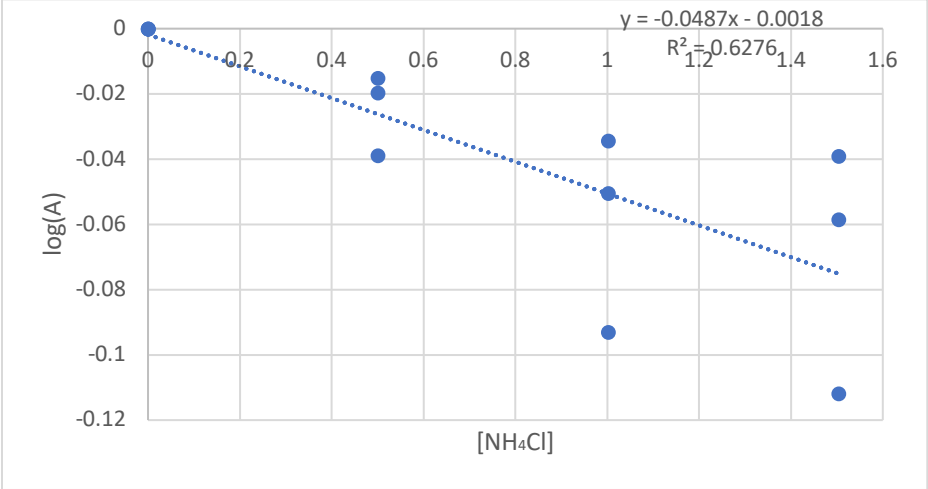

Figure 61. log(A) vs. [NH_4Cl] for 2-pentanone.

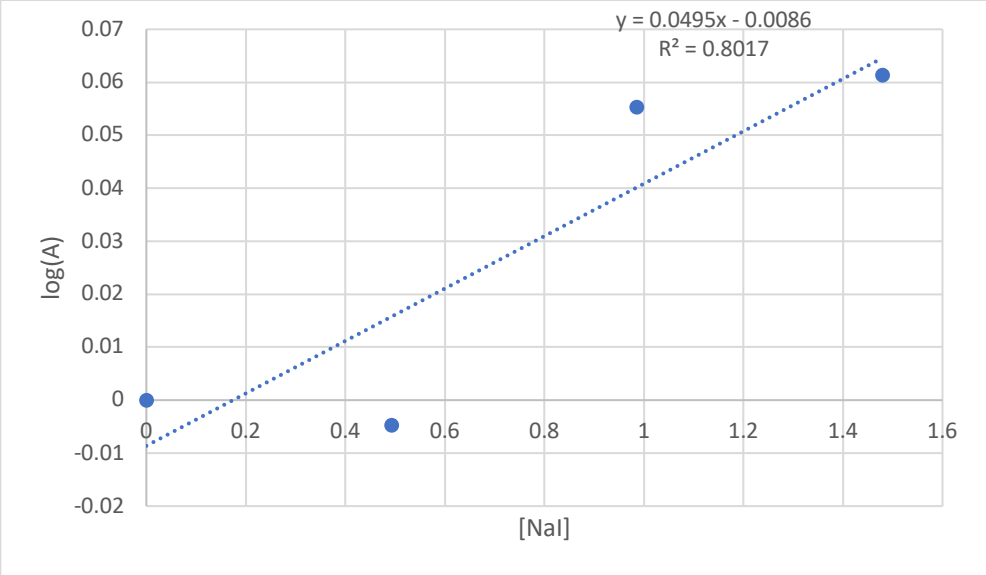

Figure 62. log(A) vs. [NaI] for 2-pentanone.

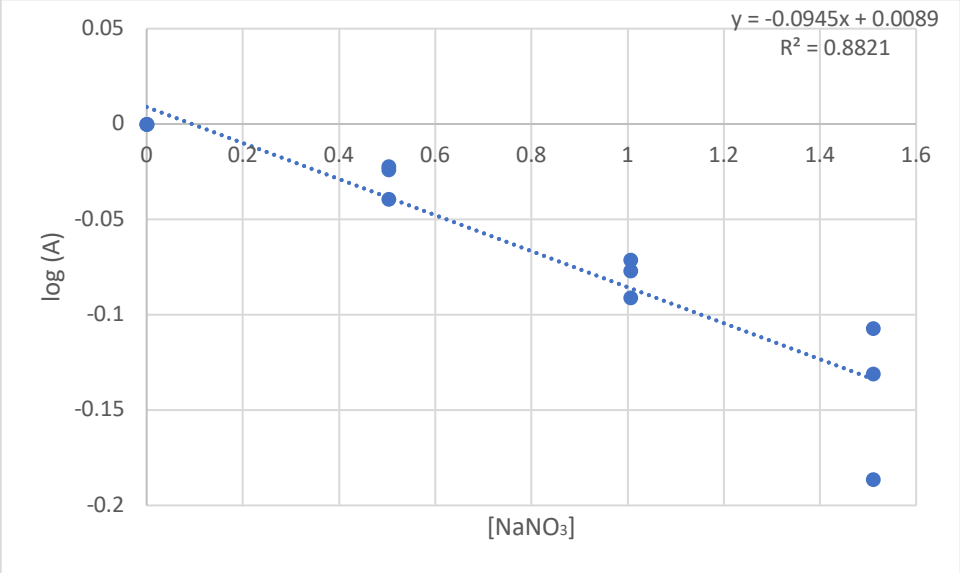

Figure 63. log(A) vs. [$NaNO_3$] for 2-pentanone.

Chlorobenzene

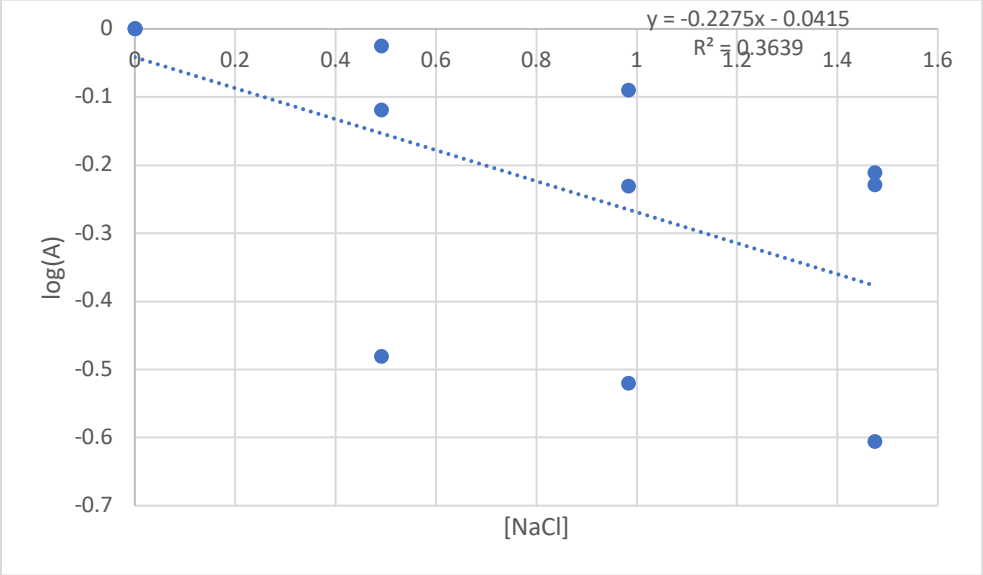

Figure 64. log(A) vs. [NaCl] for chlorobenzene.

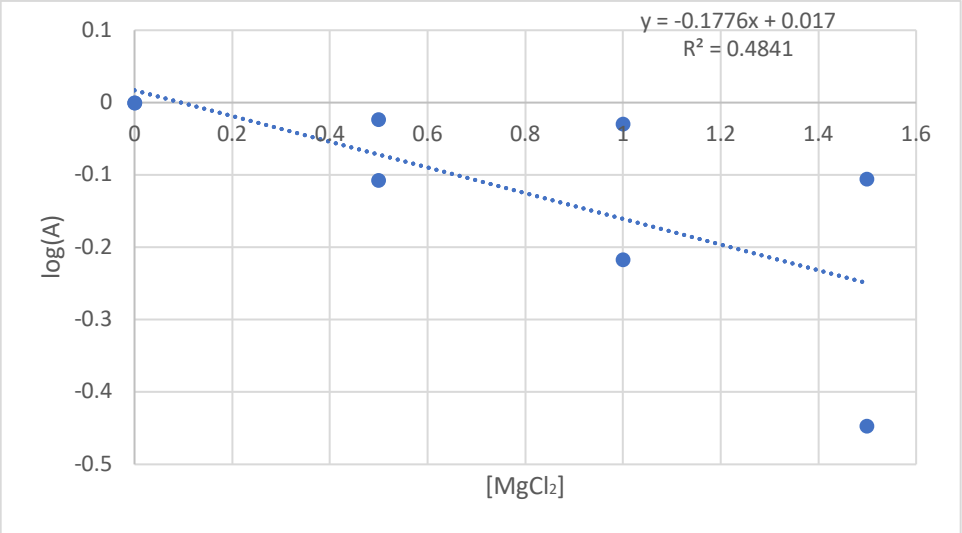

Figure 65. log(A) vs. [$MgCl_2$] for chlorobenzene.

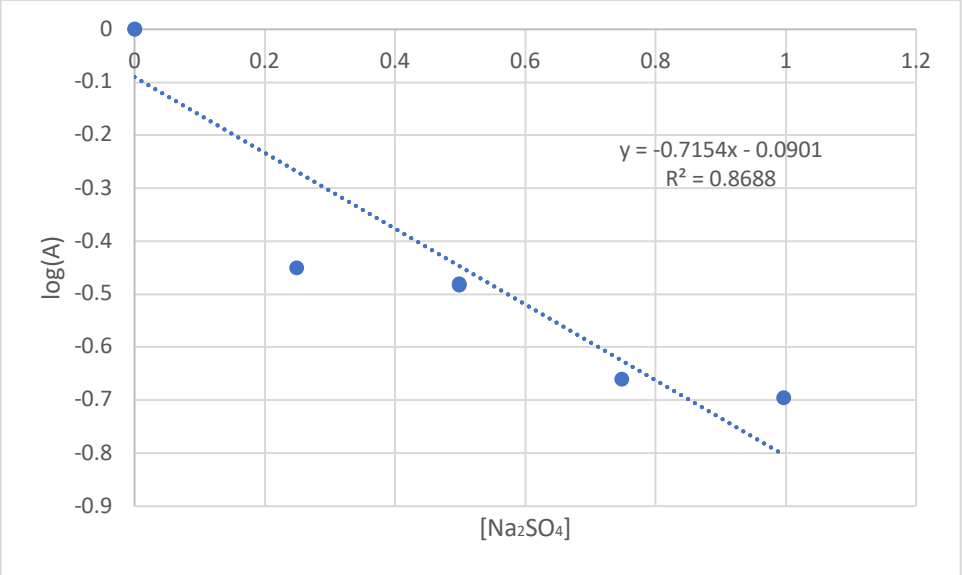

Figure 66. log(A) vs. [Na_2SO_4] for chlorobenzene.

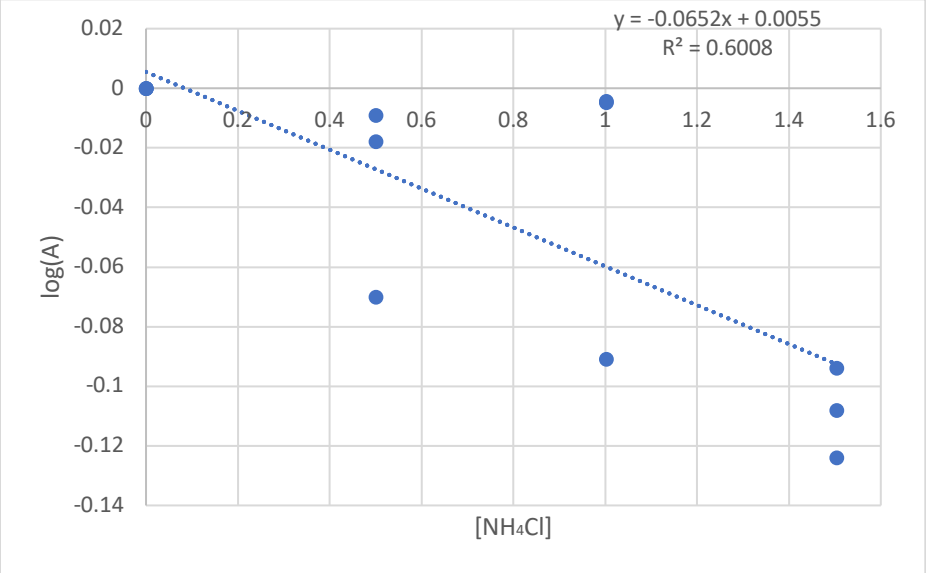

Figure 67. log(A) vs. [NH_4Cl] for chlorobenzene.

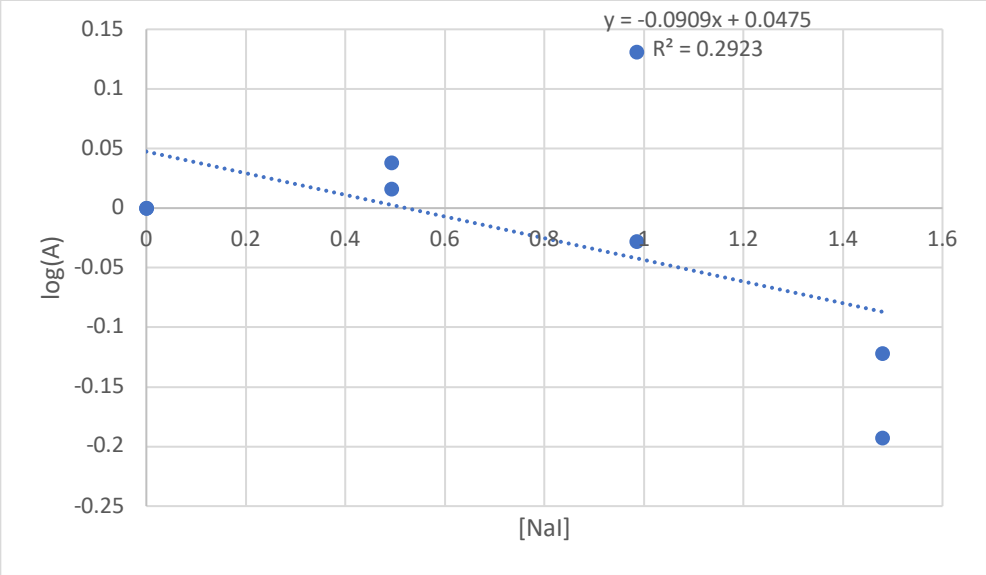

Figure 68. log(A) vs. [NaI] for chlorobenzene.

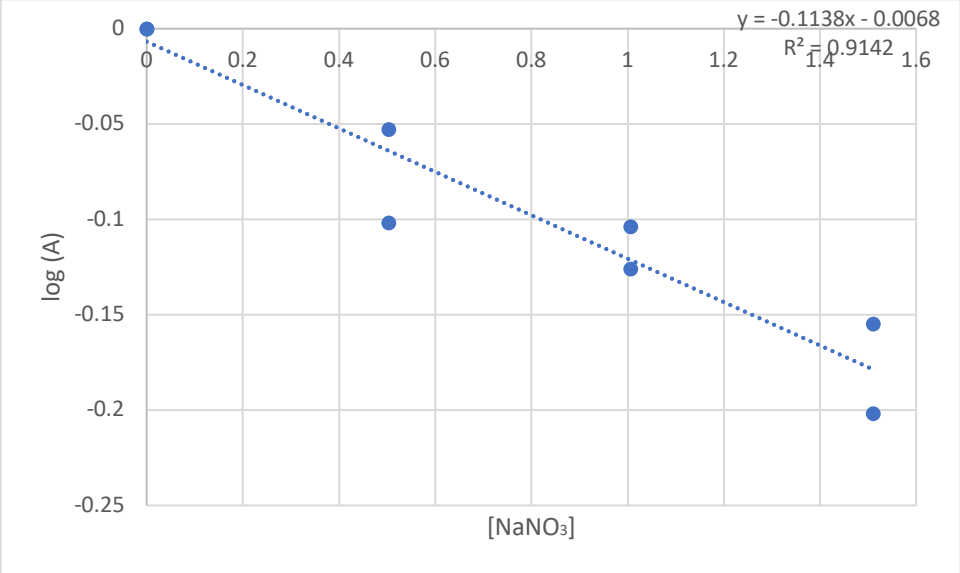

Figure 69. log(A) vs. [$NaNO_3$] for chlorobenzene.

Benzaldehyde

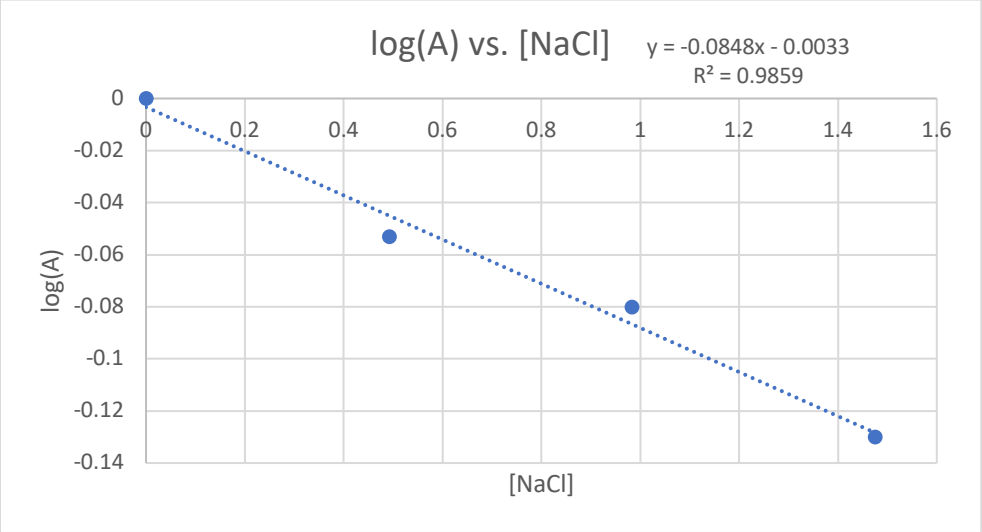

Figure 70. log(A) vs. [NaCl] for benzaldehyde.

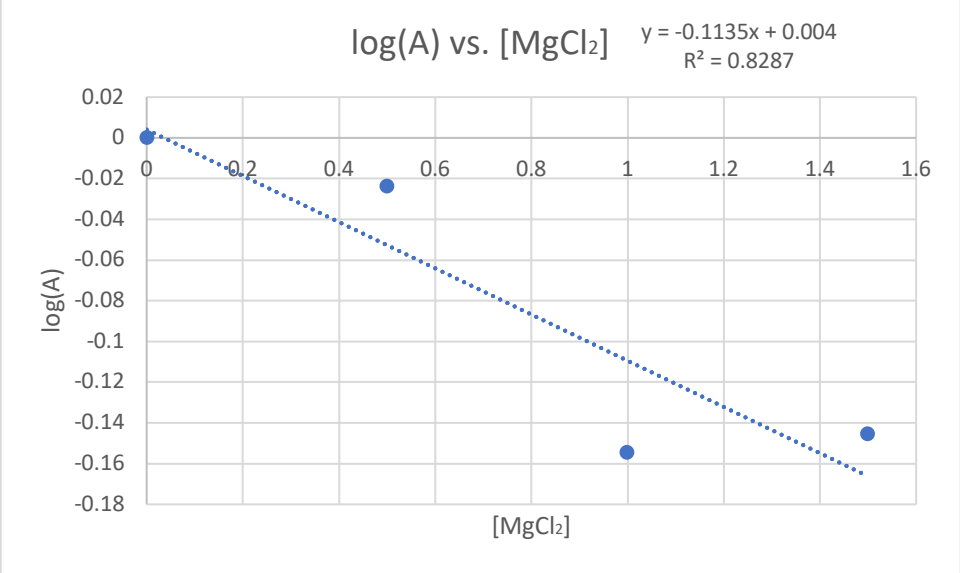

Figure 71. log(A) vs. [$MgCl_2$] for benzaldehyde.

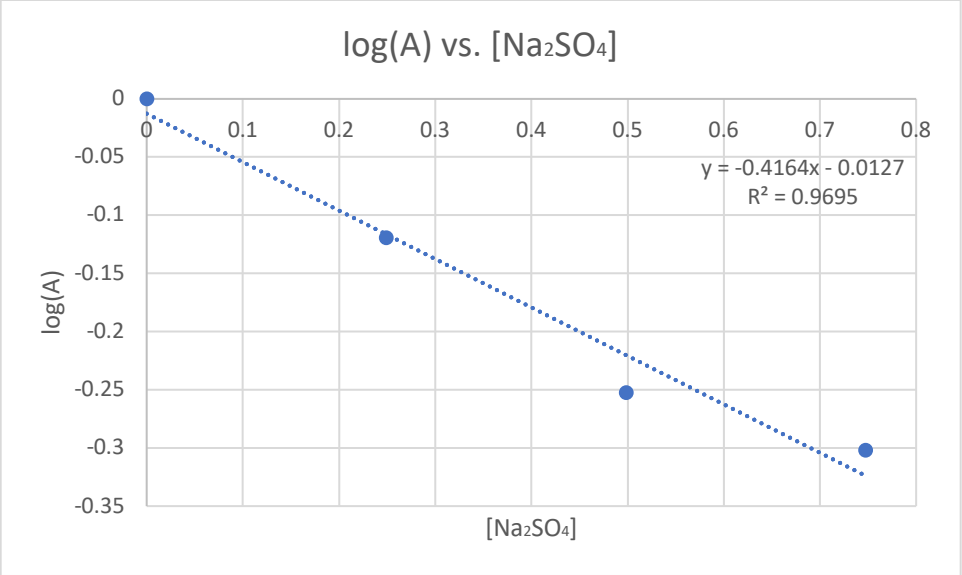

Figure 72. log(A) vs. [Na_2SO_4] for benzaldehyde.

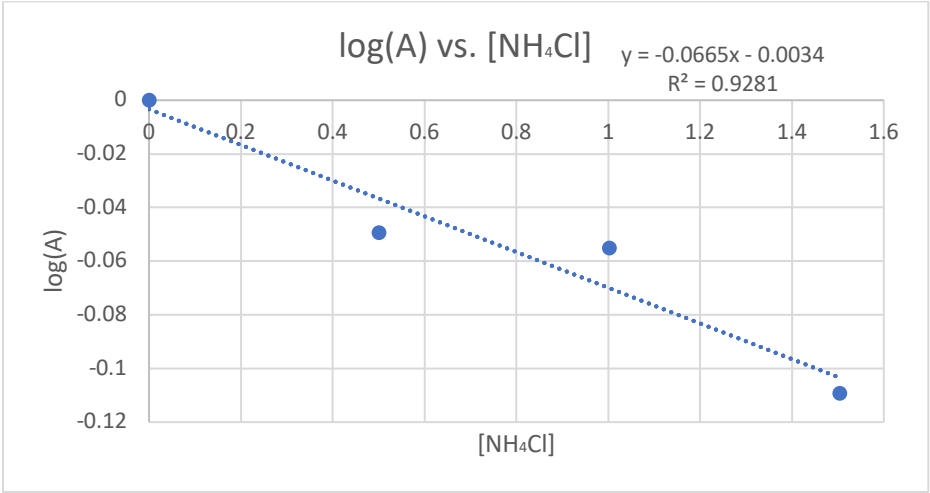

Figure 73. log(A) vs. [NH_4Cl] for benzaldehyde.

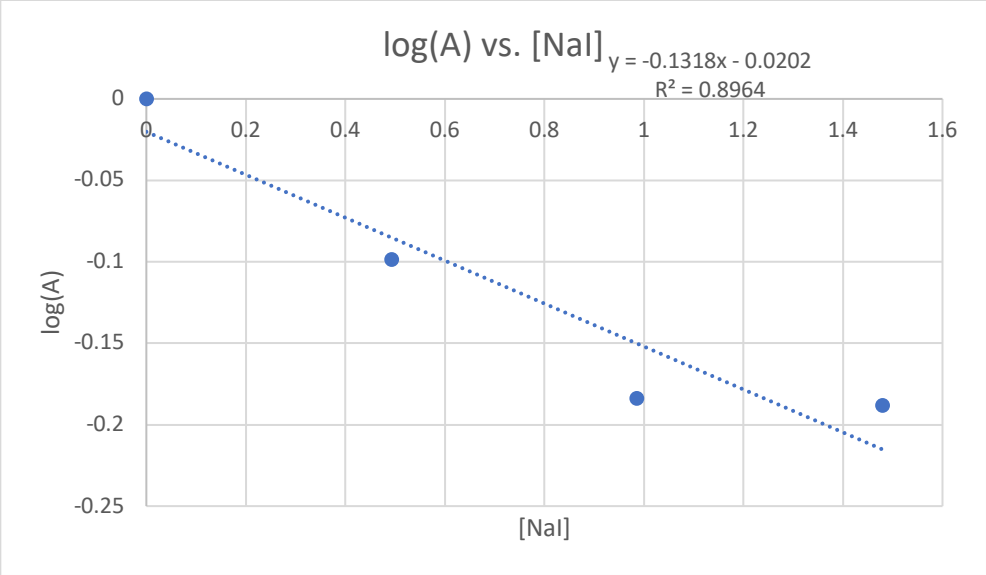

Figure 74. log(A) vs. [NaI] for benzaldehyde.

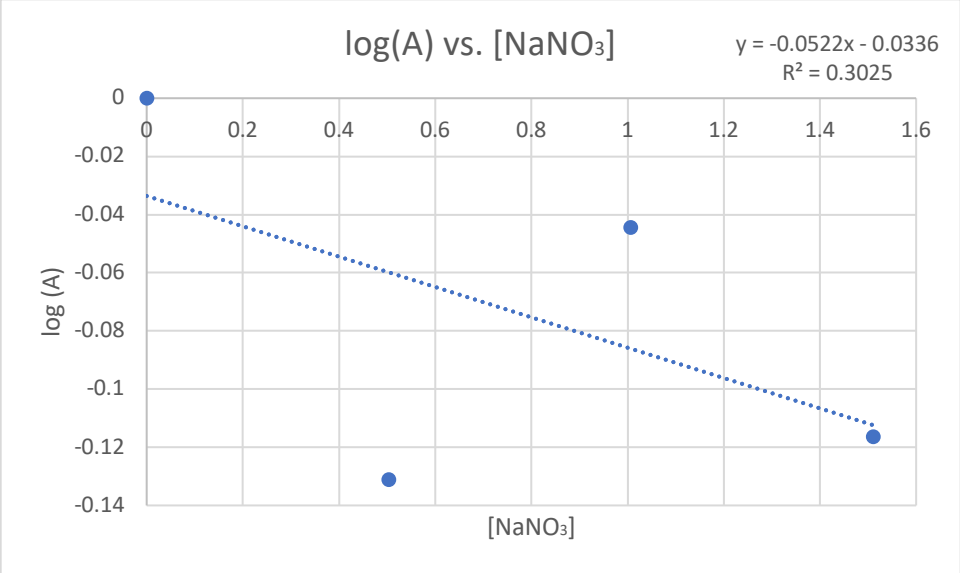

Figure 75. log(A) vs. [$NaNO_3$] for benzaldehyde.